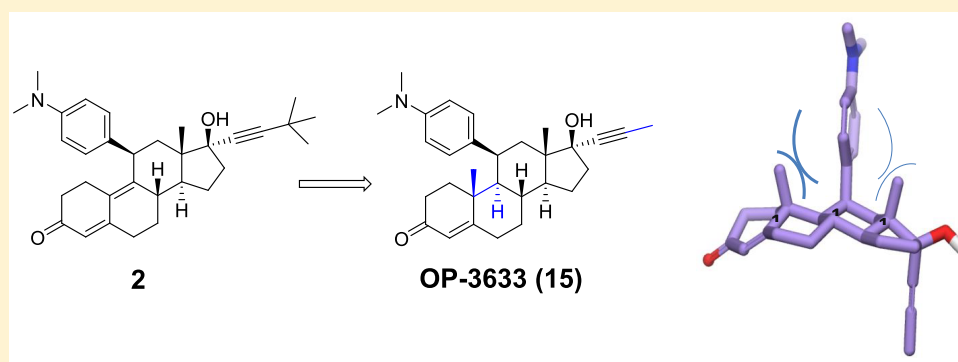


Discovery of a Potent Steroidal Glucocorticoid Receptor Antagonist with Enhanced Selectivity against the Progesterone and Androgen Receptors (OP-3633)

Xiaohui Du,^{*†} John Eksterowicz, Haiying Zhou, Yosup Rew,[†] Liusheng Zhu, Xuelei Yan, Julio C. Medina, Tom Huang, Xi Chen, Dena Sutimantanapi, Nadine Jahchan, Wayne Kong, Jessica Sun, Tatiana Zavorotinskaya, Qiuping Ye, Valeria R. Fantin, and Daqing Sun^{*}

ORIC Pharmaceuticals, 240 E. Grand Avenue, FL2, South San Francisco, California 94080, United States

Supporting Information



ABSTRACT: Structure-based modification of mifepristone (1) led to the discovery of novel mifepristone derivatives with improved selectivity profile. Addition of a methyl group at the C10 position of the steroid has a significant impact on progesterone receptor (PR) and androgen receptor (AR) activity. Within this series, OP-3633 (15) emerged as a glucocorticoid receptor (GR) antagonist with increased selectivity against PR and AR, improved cytochrome P450 inhibition profile, and significantly improved pharmacokinetic properties compared to 1. Furthermore, 15 demonstrated substantial inhibition of GR transcriptional activity in the GR positive HCC1806 triple negative breast cancer xenograft model. Overall, compound 15 is a promising GR antagonist candidate to clinically evaluate the impact of GR inhibition in reversal or prevention of therapy resistance.

INTRODUCTION

The glucocorticoid receptor (GR) is a member of the superfamily of nuclear hormone receptors that are activated by both natural and synthetic glucocorticoids (GCs), such as cortisol and dexamethasone, respectively.¹ The GR is expressed across a variety of tissues.² Upon ligand binding, GR translocates into the nucleus, where it binds to glucocorticoid response elements (GREs) and other transcription factors such as NF- κ B and AP1 to regulate the transcription of a wide range of genes controlling metabolism, cell growth, differentiation, apoptosis, inflammation, and nervous system activities, including cognition and mood.³

Given the plethora of biological processes regulated by GCs, dysregulation in receptor signaling has been implicated in a number of disease states including Cushing's syndrome,⁴ diabetes,⁵ depression,⁶ cancer,⁷ and immunosuppression.⁸ Accordingly, there has been considerable interest in the development of GR antagonists for therapeutic purposes.⁹ For example, mifepristone (1), a potent steroidal GR antagonist, was approved by the FDA in 2012 for the treatment of Cushing's

syndrome.¹⁰ More recently, GR has been shown to play a role in mediating resistance to chemotherapy in a variety of solid tumors¹¹ including ovarian cancer,¹² triple-negative breast cancer (TNBC),¹³ pancreatic cancer,¹⁴ non-small-cell lung cancer,¹⁵ and urological cancers.¹⁶ In prostate cancer, GR has been shown to create a bypass to the related androgen receptor (AR) and to drive resistance to antiandrogens such as enzalutamide and apalutamide.^{17,18} Therefore, the ability of GR antagonists, including 1, to overcome resistance to numerous standard of care agents is under clinical evaluation.

For example, the combinations of 1 with enzalutamide and nab-paclitaxel are being evaluated in castration-resistant prostate cancer (CRPC)¹⁹ and TNBC,²⁰ respectively. However, 1 exhibits partial AR agonistic activity and potent progesterone receptor (PR) antagonistic activity (IC₅₀ = 0.4 nM, Figure 1).^{21,22} More specifically, the AR agonistic activity of 1 is sufficient to stimulate the proliferation of CRPC LNCaP/AR-

Received: April 30, 2019

Published: June 25, 2019

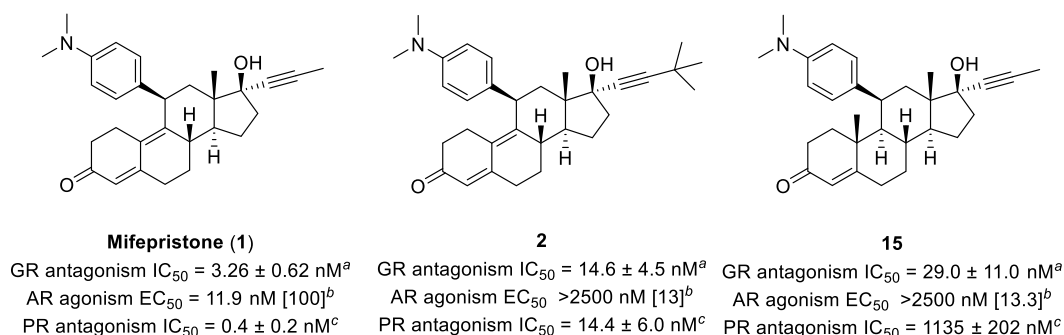


Figure 1. Mifepristone (1), compound 2, and 15. ^a IC_{50} in GR luciferase antagonist assay. ^b EC_{50} [E_{max}]^{*} in AR luciferase agonist assay. ^{*} = % mifepristone. ^c IC_{50} in PR luciferase antagonist assay.

Table 1. Exploration of Analogs of 2^a

Compound	Structure	GR luc. antagonism IC_{50} (nM)	AR luc. agonism EC_{50} (nM) [E_{max}] ^b	AR luc. antagonism IC_{50} (nM)	PR luc. antagonism IC_{50} (nM)
2		14.6±4.5	>2500 [13]	129±49	14.4±6.0
3		5.6±2.4	224±97 [22]	165±14	3.4±0.2
4		13.9±9.4	>2500 [9.4]	263±62	6.0±2.4
5		10.3±6.5	>2500 [5.1]	208	4.8±0.6
6		35.8±2.8	>2500 [7.9]	1005±407	25.4±11.1
7		12.2±1.1	>2500 [18.1]	359±47	4.6±2.6
8		12.7±9.9	>2500 [7.3]	175±9.9	21.1±11.4

^aPotency and E_{max} data with SD are reported as the average of at least two determinations. ^b% mifepristone.

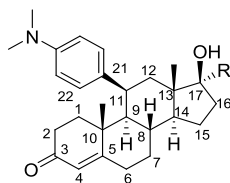
luc (LNAR) cells both in vitro and in vivo and induces AR target gene expression in AR⁺ TNBC MDA-MB-453 cells.²³ In addition, because of its CYP450 inhibition profile, when co-dosed with paclitaxel, **1** increases the paclitaxel exposure due to CYP2C8-driven drug–drug interactions.²⁰ These unwanted features of **1** limit its potential use in certain settings such as AR-driven cancers or in combinations that include paclitaxel and related chemotherapeutic agents and highlight the need for selective and potent GR antagonists that do not carry the AR, PR, and CYP2C8 liabilities of **1**.

Recently, we reported the discovery of compound **2**, a potent steroidal GR antagonist.²⁴ Introducing a *tert*-butyl group

substitution onto the alkyne moiety attenuated the AR agonism associated with **1**. Here we report the continued investigation of **1**, which led to the discovery of a series of novel C10-methyl steroidal GR antagonists. Among them, OP-3633 (**15**) exhibits lower AR agonism and excellent selectivity against GR over PR, as well as an improved CYP inhibition profile compared to **1** (Figure 1).

RESULTS AND DISCUSSION

Starting from **2**, reduction of the C9–C10 double bond in **2** led to the synthesis of **3**, which was more potent against GR but also showed a slight increase of AR agonism compared to **2**. Both **2**

Table 2. Exploration of the Alkyne Substituents at the C17 Position in the β -C10-Methyl Analogs^a

Compound	R	GR luc. antagonism IC ₅₀ (nM)	AR luc. agonism EC ₅₀ (nM) [E _{max}] ^b	AR luc. antagonism IC ₅₀ (nM)	PR luc. antagonism IC ₅₀ (nM)
9		33.6±8.5	>2500 [7.4]	>5000	2488±195
10		62.0±12.2	>2500 [8.3]	>5000	2084±359
11		28.5±6.3	>2500 [5.4]	1452±526	1487±508
12		116±13.3	>2500 [17.5]	>5000	4242±411
13		73.7±32.4	>2500 [13.2]	2955±339	1546±170
14		47.2±11.7	>2500 [7.3]	642±7	910±242
15		29.0±11.0	>2500 [13.3]	912±403	1135±202

^aPotency and E_{\max} data with SD are reported as the average of at least two determinations. ^b% mifepristone.

and **3** had lower affinity for PR compared to **1** (IC₅₀ = 14.4 and 3.4 nM, respectively), resulting in a slightly better PR/GR ratio. Several more analogs of **3** with various aniline *N*-alkyl substituents at the C11 position were synthesized with the goal of evaluating their interactions with PR (Table 1, compounds 4–7) while taking advantage of the increased potency on GR antagonism as a result of the reduced C9–C10 double bond. Luciferase (luc.) GR, AR, and PR reporter assays were employed to characterize agonism and antagonism of compounds. None of the tested compounds showed meaningful GR and PR agonism, and data for these assays are not reported in the tables below. Increase of the substituent's size to *N,N*-diethyl group (**4**) attenuated AR agonism (E_{\max} = 9.4% of **1**) and maintained high GR antagonism; however, it did not improve selectivity against PR. Replacing *N,N*-dimethyl group with a more constrained morpholine moiety (**5**) maintained GR antagonism and low AR agonism but had no impact on PR selectivity. The 4-methylpiperazinyl substitution on compound **6** weakened PR affinity (IC₅₀ = 25.4 nM) compared to **1** and **2**. However, this modification also decreased GR antagonism slightly, with no net change in PR selectivity. Replacement of the 4-dimethylamino group with the electron-withdrawing 4-(methylsulfonyl)piperazinyl group led to **7**, which was potent against GR (IC₅₀ = 12.2 nM) and PR (IC₅₀ = 4.6 nM). Installing a 3,3-dimethylpentynyl group, slightly bulkier than *tert*-butyl group at the C17 position (**8**), diminished the GR inhibition potency (IC₅₀ = 12.7 nM) to a lesser extent than the PR inhibition potency (IC₅₀ = 21.1 nM) compared to **3** and resulted in a small improvement in the selectivity against PR compared to **1**, **2**, and **3**. Overall, the compounds shown in Table 1 have lower affinity for PR compared to **1** but have no significant improvement in PR selectivity compared to **2**. Compounds in Table 1 were also tested for their AR antagonistic activity, and

their IC₅₀ values are shown in the table. These compounds are moderate to weak AR antagonists, resulting in a 10- to 30-fold GR over AR selectivity.

In the literature, it has been noted that the β -C10-methyl group on the androstene steroid can weaken the affinity toward PR.²⁵ The hypothesis is that the steric interaction between the β -C10-methyl group and the β -C11-aryl moiety results in ring A bending downward compared to the corresponding analog with a C9–C10 double bond (when using C7, C11, and O17 as anchor positions), and the displacement of the carbonyl functional group leads to the low affinity for PR. We decided to introduce the β -C10-methyl group into our existing GR antagonists to evaluate its impact on PR, GR, and AR interactions. Table 2 shows a number of β -C10-methyl analogs with various propynyl groups at the C17 position (compounds 9–15) while maintaining 4-dimethylaminophenyl substitution at C11. With a methyl substitution at the C10 position, compound **9** showed a reduction in AR agonism (E_{\max} = 7.4% of **1** for **9** compared to E_{\max} = 22% of **1** for **3**) and a 6-fold decrease in GR antagonism compared to its C10-hydrogen analog **3** (IC₅₀ = 33.6 nM for **9** and IC₅₀ = 5.6 nM for **3**). Strikingly, compound **9** was found to have a much-weakened PR affinity (IC₅₀ = 2.5 μ M), which was significantly lower than that of **3** (IC₅₀ = 3.4 nM) and led to a 70-fold GR over PR selectivity.

Encouraged by the increased PR selectivity of **9**, we next explored whether small alkyne substitutions at the C17 position would improve GR antagonism while maintaining PR selectivity. Changing the *tert*-butyl group to smaller alkyl groups maintained high selectivity against PR (Table 2). The PR antagonist IC₅₀ of **10**–**15** ranged from 0.91 μ M to 4.24 μ M. Interestingly, decrease of the substituent's size from a *tert*-butyl group to a methyl group triggered no substantial AR agonism (**9** vs **15**). All of the C10-methyl analogs had remarkably decreased AR agonism

compared to their corresponding C9–C10 double bond analogs reported by us previously.²⁴ For example, compound **10** with an isopropyl alkyl substitution at C17 showed low AR agonism (E_{\max} = 8.3% of **1**), while the corresponding C9–C10 double bond analog had much higher AR agonism (E_{\max} = 50% of **1**). Similarly, compound **15** with a methyl group substitution had low AR agonism (E_{\max} = 13.3% of **1**), while the corresponding C9–C10 double bond analog **1** exhibited maximum AR agonism (E_{\max} = 100%). These results imply that a methyl group at the C10 position is crucial to minimize AR agonism and PR antagonism and that a large *tert*-butyl group is not required to attenuate AR agonism of the C10-methyl analogs. Furthermore, most of the C10-methyl analogs in Table 2 are much weaker AR antagonists compared to those in Table 1. On the other hand, the C10-methyl compounds in Table 2 suffer from loss of GR antagonism at various degrees. Among them, compounds **9**, **11**, and **15** were most potent (IC_{50} from 28 nM to 34 nM), within 2-fold difference compared to **2**.

In addition to the GR IC_{50} values shown in Tables 1 and 2, Figure 2 shows the dose–response curves for the luciferase assay

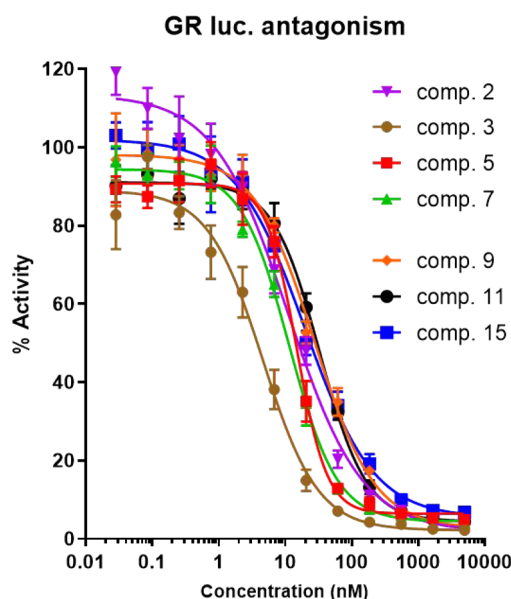


Figure 2. Dose–response curves for the GR luciferase assay of selected compounds in Table 1 and Table 2.

of several most potent GR antagonists in each table using compound **1** (mifepristone) as control. All of them can completely inhibit the activity of GR, demonstrating that they are GR full antagonists.

To elucidate the structural basis for the improved PR selectivity observed upon the addition of a methyl group at C10, a variety of approaches were undertaken. Consistent with earlier observations, modeling studies suggested that reduction of the C9–C10 double bond would change the shape of the scaffold.²⁵ In addition, ab initio calculations showed that the β -C10-methyl group has a significant effect on the rotational profile of the β -C11 4-dimethylaminophenyl group, restricting the C₉–C₁₁–C₂₁–C₂₂ rotation (Figure 3) such that the plane of the phenyl ring is essentially fixed, sandwiched between the C10 and C13 methyl groups.

Finally, small molecule X-ray structures of both **1** and **15** were obtained. As shown in Figure 4, the data are consistent with the results from the ab initio calculations. (A) shows the structure of

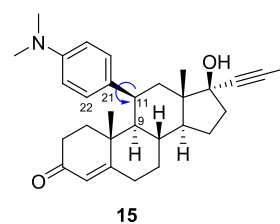


Figure 3. Illustration of C₉–C₁₁–C₂₁–C₂₂ rotation.

1 (green), in which the A–B–C–D rings of the scaffold adopted a relatively flat orientation with a slight twist of the C₉–C₁₁–C₂₁–C₂₂ torsional angle of 15.4°. In comparison, (B) shows the structure of **15** (purple) in the same orientation. The puckering of the scaffold is evident and may affect the ability of the A-ring carbonyl to make a key hydrogen bond interaction present in PR, AR, and GR. Furthermore, the addition of the β -C10-methyl group causes rotation of the C₉–C₁₁–C₂₁–C₂₂ bond to 38.4°. This forced change in the conformation may result in additional steric conflicts with PR, resulting in improved selectivity toward GR.²⁶ (C) shows the overlay of the two structures further highlighting the key differences.

Inspired by the discovery of the β -C10-methyl analogs, we further investigated modification of the aryl group at the C11 position to improve GR antagonism. Bulkier substitutions were introduced to the aryl group, and their functional impact was assessed. Replacement of one of the *N*-methyl groups on the 4-dimethylaminophenyl in **15** with an isopropyl group (**16**) improved GR antagonism (IC_{50} = 20.6 nM) and also maintained good selectivity against PR. However, compound **16** had an unexpected higher AR agonism (E_{\max} = 55.9% of **1**). Expanding the 4-dimethylaminophenyl to an *N*-methyl-*N*-methoxyethylphenyl (**17**) restored low AR agonism and maintained high selectivity against PR. However, compound **17** was a less potent GR antagonist compared to **15**. Replacing the 4-dimethylaminophenyl with a constrained substituent 4-pyrrolidinylphenyl (**18**) did not improve its GR antagonistic potency. Similarly, changing the 4-dimethylaminophenyl to a 4-pyrrolylphenyl (**19**) provided no improvement in GR antagonism. A bigger change resulting from the replacement of the C11 aniline by a 4-methoxyphenyl (**20**) did not improve the GR potency either.

We noted that one GR antagonist recently reported in the literature carries a 4-chlorobenzoyloxy group at C11.²⁷ To determine the impact of this group on our scaffold, 4-chlorobenzoyloxy group was introduced at C11. **21** had improved GR antagonism (IC_{50} = 17.6 nM) but showed a significant decrease in selectivity against PR (IC_{50} = 8.2 nM) as well as a significant increase in AR agonism (E_{\max} = 47.8%) and AR antagonism (IC_{50} = 85 nM) (Table 3). These results suggest that the reduced steric clash between the β -C10-methyl group and the β -C11 4-chlorobenzoyloxy moiety in **21** is not able to hold the conformation required for the reduced affinity toward PR.

Given the GR antagonistic potency, high selectivity against PR, and low AR agonism, compounds **9**, **11**, and **15** were selected for evaluation in the CYP inhibition assays (Table 4). The results from those studies showed that compound **15** had relative low potential for CYP3A4 and CYP2C8 inhibition compared to **9** and **11** at the concentration of 10 μ M.

Since compound **1** was reported to have high potential for CYP2C8 inhibition (IC_{50} = 1.5 μ M), a detailed CYP IC_{50} evaluation of **15** was performed in comparison to **1** and **2**. As shown in Table 5, compound **2** had a much lower potential for

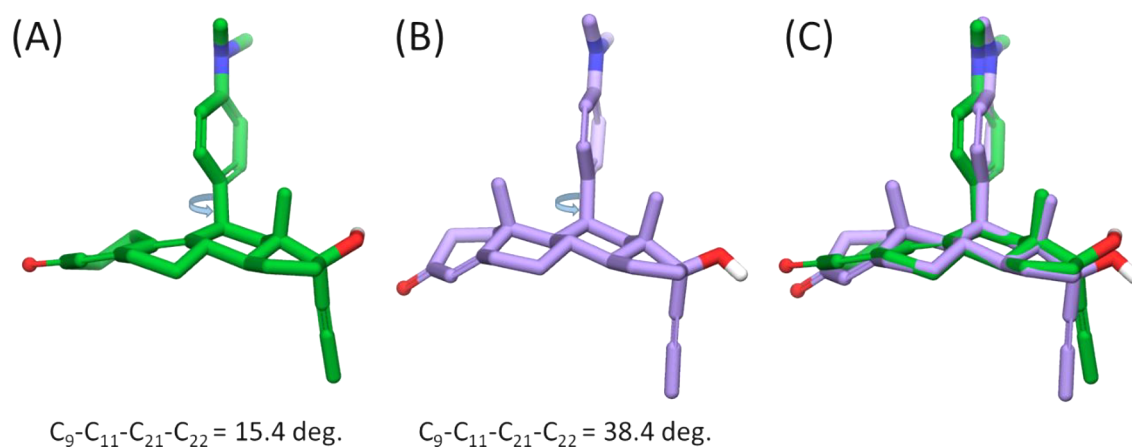


Figure 4. Comparison of the small molecule X-ray structures of mifepristone (A, green) with **15** (B, purple) with key torsional angle highlighted. The overlay of the two structures is shown in (C).

Table 3. Modification of the Substituents at the C11 Position^a

Compound	Structure	GR luc. Antagonism IC_{50} (nM)	AR luc. agonism EC_{50} (nM) [E_{max}] ^b	AR luc. antagonism IC_{50} (nM)	PR luc. antagonism IC_{50} (nM)
16		20.6±6.6	1142 [55.9]	2246±217	527±126
17		52.1±3.5	>2500 [20.0]	1295±160	1640±220
18		57.9 ±24.5	>2500 [10.6]	3146±2622	4068±1614
19		52.2±16.4	>2500 [16.5]	354±87	523±257
20		58.3±27.0	>2500 [14.1]	561±93	1689±125
21		17.6±12.8	1885 [47.8]	85±21	8.2±3.8

^aPotency and E_{max} data with SD are reported as the average of at least two determinations. ^b% mifepristone.

Table 4. CYP Inhibition of Compounds 9, 11, and 15

P450 isoform	substrate	% inhibition (10 μ M)		
		9	11	15
3A4	midazolam	71	53	34
2C8	paclitaxel	84	70	58

Table 5. CYP Profiles of 1, 2, and 15^a

P450 isoform	substrate	IC ₅₀ (μ M)		
		1	2	15
3A4	midazolam	9.5 ^b	2.9 ^c	>10 ^d
2C8 ^e	paclitaxel	1.5	>10	8

^aCYP2C8 and CYP3A4 data are reported as the average of at least two determinations. ^bIC₅₀ is between 8.1 and 13 μ M ($n = 8$). ^cIC₅₀ is between 2.4 and 3.4 μ M ($n = 2$). ^dIC₅₀ is >10 μ M each time ($n = 2$). ^eCYP2C8 IC₅₀ for compounds 1, 2, 15 is within 10% of average value in each measurement.

CYP2C8 inhibition but elevated CYP3A4 inhibition relative to compound 1. Compound 15 offered an improved overall profile with low inhibition potential for both CYP3A4 and CYP2C8.

Next, compound 15 was subjected to further in vitro profiling. In the PolarScreen glucocorticoid receptor competitor assay (Figure 5), the potency of compound 15 (IC₅₀ = 8.5 nM was

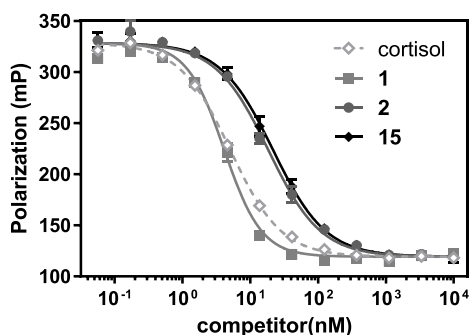


Figure 5. Binding affinities of 1, 2, and 15 to human GR in the PolarScreen GR competitor assay.

comparable to that of 2 (IC₅₀ = 8.0 nM) and 3.5-fold lower than that of 1 (IC₅₀ = 2.3 nM). In the GR-coactivator interaction assay (Figure 6), compound 15 was 2-fold less potent than 2 (IC₅₀ = 16 nM and IC₅₀ = 7.5 nM, respectively) and approximately 4.5-fold less potent than 1 (IC₅₀ = 3.5 nM).

To determine whether 15 would be suitable for preclinical development, its pharmacokinetic properties were characterized

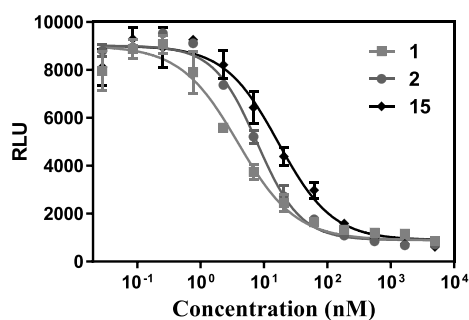


Figure 6. 2 and 15 block the interaction between GR and its coactivator in the GR-coactivator protein-protein interaction assay.

in preclinical species, namely, rat, dog, and mini-pig. Although compound 15 had similar clearance to that of 1 and 2 in rat, it showed about 10-fold and 2-fold higher oral exposure than that of 1 and 2, respectively (Table 6). Additionally, compound 15

Table 6. Pharmacokinetic Data of 1, 2 and 15 in Rat

compd	iv (0.5 mg/kg) ^a			po (5 mg/kg)		
	CL (L kg ⁻¹ h ⁻¹)	V _{ss} (L/kg)	t _{1/2} (iv, h)	F (%)	C _{max} (μ g/L)	AUC (μ g·h/L)
1 ^b	3.7	4.1	1.6	6.4	24	85
2 ^b	4.0	4.9	1.9	37	72	471
15 ^c	3.1	4.7	1.8	62	518	1020

^aFormulated in 10% DMSO, 70% PEG 400, and 20% water. ^bFormulated in 5% DMSO, 95% 0.2% Tween 80 in 0.25% CMC. ^c5% DMSO/95% 0.2% Tween 80 in 0.25% CMC, pH 4.

had moderate clearance and good oral exposure in both dog and mini-pig (Table 7). The favorable solubility of 15 (Table 8) across all pH levels might contribute to the high oral exposures across species.

Table 7. Pharmacokinetic Data of 15 in Dog and Mini-Pig

species	iv (0.5 mg/kg) ^a			po (5 mg/kg) ^b		
	CL (L kg ⁻¹ h ⁻¹)	V _{ss} (L/kg)	t _{1/2} (h)	F (%)	C _{max} (μ g/L)	AUC (μ g·h/L)
dog	0.61	8.32	16.2	67.6	1261	5927
mini-pig	0.75	1.45	2.71	35.9	249	2451

^a15 was in 5% DMA, 10% EtOH, 40% PEG400, and 45% DSW for iv study. ^b15 was in 95% 0.2% Tween 80, and 5% DMSO in 0.25% CMC, for dog oral study, and 15 was in 95% 0.2% Tween 80, and 5% DMSO in 0.25% CMC, pH 4 for mini-pig oral study.

Table 8. Solubility of Compounds 1 and 15

compd	solubility (μ M)		
	FaSSGF	FaSSIF	PBS
	pH 1.2	pH 6.5	pH 7.4
1	>1164	5.4	3.0
15	1130	59.5	20.6

Furthermore, we evaluated whether 15 could inhibit GR transcriptional activity in the HCC1806 xenograft model. A bolus oral dose of cortisol (5 mg/kg) was administered to effectively activate human GR in HCC1806 triple negative breast cancer cells. Expression of the GR target gene FKBP5 was analyzed in HCC1806 tumors collected from mice at 3 and 6 h after cortisol administration, receiving either a single oral dose of 15 or vehicle as a control. Cortisol treatment resulted in 2.3- to 4.0-fold induction of FKBP5 expression compared to the vehicle group, assessed by RT-qPCR. In the presence of 15 at 150 mg/kg, cortisol-mediated induction of FKBP5 expression was reduced 2.8-fold and 2.3-fold, respectively. The levels of FKBP5 in tumors from mice treated with 15 and cortisol at both 3 and 6 h were comparable to those detected in tumors from the vehicle treated mice (Figure 7A). The unbound plasma concentration of 15 reached 400 nM at 1 h and remained at that level during the study period (Figure 7B). These data suggest that 15 is effective at inhibiting cortisol-induced GR target gene expression in HCC1806 xenograft tumors, and the reduction of GR target gene expression could be correlated with the plasma exposure of 15.

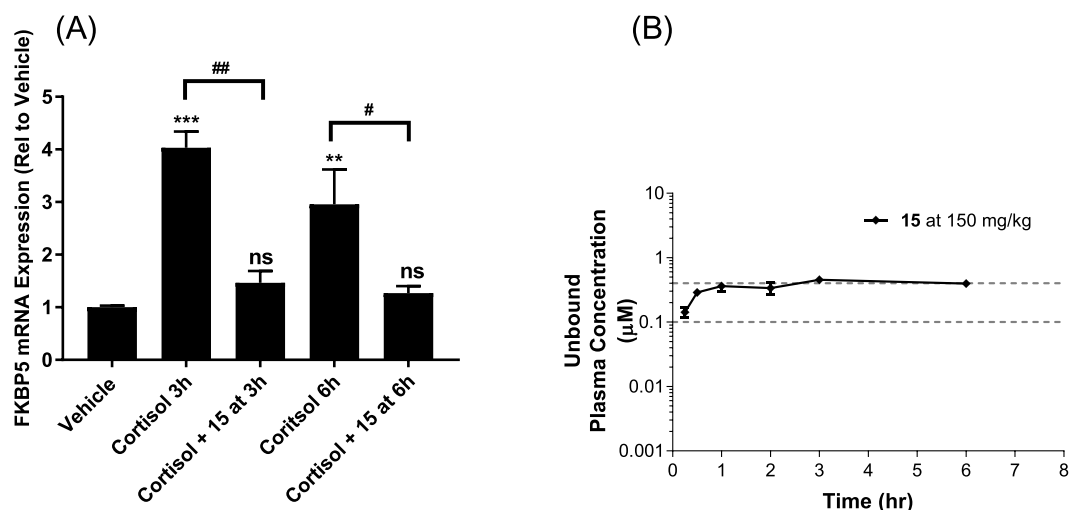


Figure 7. In vivo pharmacodynamics of compound **15**. (A) mRNA levels of GR target gene FKBP5 in HCC1806 tumors relative to vehicle 3 and 6 h after treatment ($n = 3$ mice/group). Cortisol was administered orally at 5 mg/kg. A single dose of **15** at 150 mg/kg was administered orally by gavage. (B) Unbound plasma concentration–time profile of **15** up to 6 h in group treated with cortisol at 5 mg/kg and **15** at 150 mg/kg ($n = 3$ mice per group). Significance of effects on FKBP5 expression was determined by one-way ANOVA using Dunnett's test to correct for multiple comparisons: (***) $p < 0.001$ and (**) $p < 0.01$ vs vehicle group; ns, no significant difference vs vehicle group; (##) $p < 0.01$ and (#) $p < 0.05$ vs corresponding cortisol group.

As anticipated from previous reports evaluating safety of GR antagonists such as **1**, adrenal gland enlargement and a change in uterine weight were noted.^{22,28} Since compound **15** exhibited enhanced selectivity for GR relative to PR in the luciferase assay and had high oral exposure in rat, the safety profile of **15** was explored, and particular attention was paid to the impact on the female reproductive system. We reasoned that the reduced inhibitory activity of **15** on PR could help minimize potential risks associated with inhibition of this nuclear receptor in female reproductive organs such as endometrial hypertrophy, irregular vaginal bleeding, and pain. On the basis of a 2-fold safety margin above the effective inhibition exposure of **15** (Figure 7B) on GR target gene expression in HCC1806 xenograft tumors, oral (gavage) administration of **15** once daily to rats for 14 days at the dose of 250 mg kg⁻¹ day⁻¹ was performed to determine its potential toxicity. The study revealed that **15** was well tolerated in female rats across the entire study period. There were no clinical observations and effects on mean body weights or changes in food consumption related to **15** during this study. Importantly, no noticeable **15**-related effects were observed in ovarian or uterine weight. The **15**-related findings were considered nonadverse based on minimal to mild severity and lack of clinical pathology correlates suggestive of organ dysfunction.

CHEMISTRY

Compounds **3–8** were synthesized according to the procedures reported previously.²⁴ Scheme 1 described the synthesis of **15** via a modified known synthetic route.²⁵ In a similar fashion, compounds **9–14** and **16–20** were prepared from the appropriate starting materials.

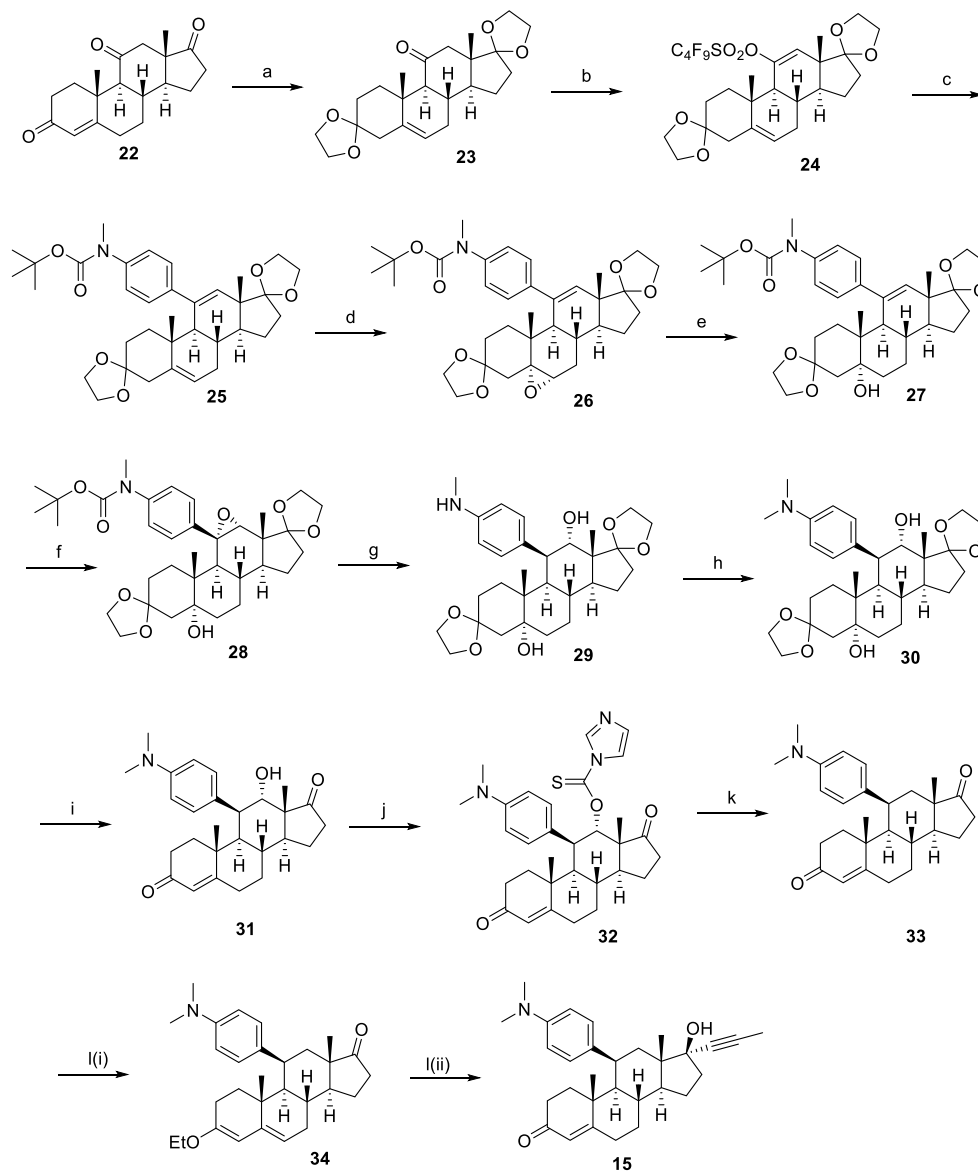
Our route toward **15** began with the conversion of adrenosterone **22** to bis-ketal **23** under acidic conditions. The carbonyl group in **23** was converted to enol nonaflate **24** via lithiation with LDA and subsequent treatment with 1,1,2,2,3,3,4,4,4-nonafluoro-1-butanefluoronyl fluoride. Suzuki coupling of **24** with Boc-protected methylaminophenylboronic acid afforded **25** exclusively. An attempt to install the desired stereochemistry at C11 via the Birch reduction in a trial reaction

resulted in the undesired stereochemistry. Alternatively, selective epoxidation²⁹ of the C5–C6 double bond with hydrogen peroxide activated by hexafluoroacetone furnished α -substituted epoxide **26**, which was reduced to alcohol **27** with lithium aluminum hydride. Oxidation of the C11–C12 double bond in **27** with *m*CPBA provided a 1:1.7 α/β mixture of epoxides, with the α -epoxide **28** as the minor diastereomer. Birch reduction of **28** yielded desired β -C11 aryl compound **29**. Fortunately, the Boc group was removed during the reaction. Reductive amination of **29** with formaldehyde enabled installation of the *N*-methyl group. Deprotection of bis-ketal on **30** and elimination of the C5 hydroxyl group in the presence of HCl gave diketone **31**. Barton deoxygenation of the C12 hydroxyl group in **31** via an imidazole carbothioate intermediate **32** provided **33**, which was then selectively protected as ethoxy dienone **34** under acidic conditions.³⁰ Finally, addition of prop-1-yn-1-ylmagnesium bromide to **34** followed by in situ deprotection of the ethoxy dienone afforded compound **15**.

The synthesis of compound **21** is illustrated in Scheme 2. Reduction of intermediate **23** with lithium aluminum hydride provided alcohol **35** as a single isomer. Alkylation of **35** with 4-chlorobenzyl bromide followed by hydrolysis with 4 N hydrochloric acid gave enone **37**, which was then protected as ethoxy dienone **38** under acidic conditions. Changing the solvent from ethanol to a mixture of THF and ethanol (30:1) minimized the formation of bis-enol ether and improved the yield of **38**.³¹ Addition of prop-1-yn-1-ylmagnesium bromide to **38** followed by in situ deprotection of the ethoxy dienone afforded the final compound **21**.

CONCLUSION

In summary, structural modification of **1** by incorporation of a methyl group at the C10 position led to the discovery of **15**, a potent, selective,³² and orally bioavailable C10-methyl GR antagonist. The enhanced selectivity for GR over PR and AR and excellent bioavailability of **15** can be rationalized by the conformation changes, which were triggered by the increased steric interaction between the C10-methyl group and the C11-aniline moiety. Those changes were observed by super-

Scheme 1. Synthesis of **15**^a

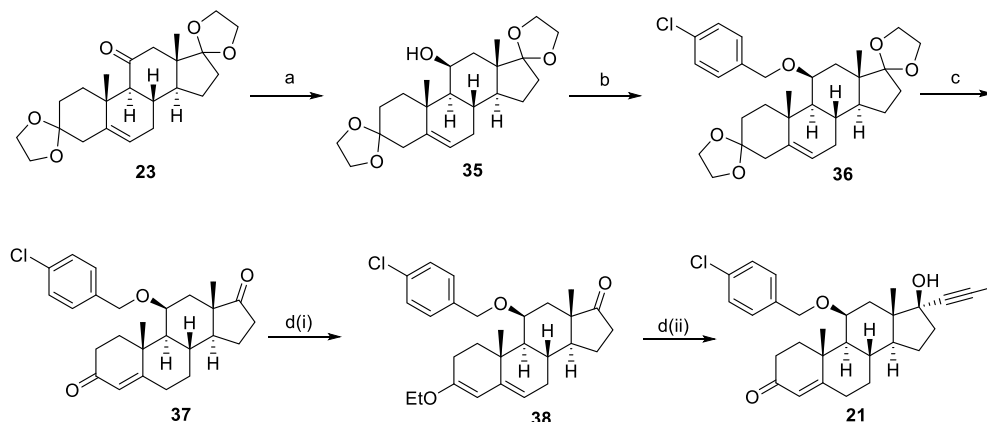
^aReagents and conditions: (a) $\text{CH}(\text{OMe})_3$, ethylene glycol, TsOH , 40°C , 18 h, 65%; (b) LDA , THF , -78°C , 30 min, then $\text{C}_4\text{F}_9\text{SO}_2\text{F}$, 2 d, 55%; (c) 4-((*tert*-butoxycarbonyl)(methyl)amino)phenyl)boronic acid, LiCl , 2 M Na_2CO_3 , toluene, ethanol, reflux, 42 h, 92%; (d) H_2O_2 , Na_2HPO_4 , CF_3COCF_3 , 2 d, 88%; (e) LiAlH_4 , THF , 1 h, 88%; (f) *m*CPBA, DCM , 20 h, 27%; (g) Li , NH_3 , THF , 81%; (h) HCHO , HOAc , DCM , $\text{NaBH}(\text{OAc})_3$, 1 h, 92%; (i) 4 N HCl , acetone, 2 h, 96%; (j) 1,1'-thiocarbonyldiimidazole, Et_3N , DCM , 4 d, 83%; (k) Bu_3SnH , toluene, reflux, 3 h, 84%; (l) (i) TsOH , $\text{CH}(\text{OEt})_3$, EtOH , 1 h, 29%; (ii) prop-1-yn-1-ylmagnesium bromide, THF , overnight, followed by 4 N HCl , 1 h, 75%.

imposition of the single crystal structures of **15** and **1**. In addition, **15** demonstrated substantial inhibition of cortisol-induced GR target gene expression in HCC1806 TNBC xenograft tumors. In a 14-day rat exploratory toxicology study, oral administration of **15** was well tolerated with no signs of PR inhibition-related effects in uterus and ovaries. The combination of GR antagonistic potency, enhanced selectivity, and superior cytochrome P450 inhibition profile, as well as suitable pharmacokinetic properties, makes compound **15** a potential candidate for the treatment of cancer in patients.

EXPERIMENTAL SECTION

General Chemistry. All reactions were conducted under an inert gas atmosphere (nitrogen or argon) with a Teflon-coated magnetic stirbar at the temperature indicated. Commercial reagents and anhydrous solvents were used without further purification. Flash

chromatography was performed on Teledyne RediSep Rf Flash silica gel columns. Removal of solvents was conducted via a rotary evaporator, and residual solvent was removed from nonvolatile compounds using a vacuum manifold maintained at approximately 1 Torr. All yields reported are isolated yields. Preparative reversed-phase high pressure liquid chromatography (RP-HPLC) was performed using an Agilent 1100 series HPLC and Phenomenex Gemini C18 column ($5\ \mu\text{m}$, $100\ \text{mm} \times 21.2\ \text{mm}$ i.d.), eluting with a binary solvent system A and B using a gradient elution [A, H_2O with 0.1% trifluoroacetic acid (TFA); B, CH_3CN with 0.1% TFA] with UV detection at 220 nm. All final compounds were purified to $\geq 95\%$ purity as determined by a Agilent 1100 series HPLC with UV detection at 220 nm using the following method: Phenomenex Gemini $5\ \mu\text{m}$ C18 110A column ($3.5\ \mu\text{m}$, $150\ \text{mm} \times 4.6\ \text{mm}$ i.d.); mobile phase, A = H_2O with 0.1% TFA, B = CH_3CN with 0.1% TFA; gradient 5–95% B (0.0–15.0 min); flow rate, 1.5 mL/min. Low-resolution mass spectral (MS) data were determined on an Agilent 1100 series LCMS with UV detection at 254 nm and a low

Scheme 2. Synthesis of Compound 21^a

^aReagents and conditions: (a) LiAlH₄, THF, 0 °C to rt, 3 h, 61%; (b) NaH, 4-Cl BnBr, 0 °C to rt, overnight, 68%; (c) 4 N HCl, acetone, 2.5 h, 86%; (d) (i) TsOH, CH(OEt)₃, THF/EtOH, 3 h, 56%; (ii) prop-1-yn-1-ylmagnesium bromide, THF, 0 °C to rt, 15 h, followed by 1 N HCl, 30 min, 76%.

resolution electrospray mode (ESI). ¹H NMR spectra were obtained on a Bruker 400 (400 MHz) spectrometer. Chemical shifts (δ) are reported in parts per million (ppm) relative to residual undeuterated solvent as an internal reference. The following abbreviations were used to explain the multiplicities: s = single; d = doublet; t = triplet; q = quartet; dd = doublet of doublets; dt = doublet of triplets; sep = septet; m = multiplet; br = broad.

Compounds 3–8 were prepared by procedures similar to those described in Scheme 3 of our previous publication.²⁴

(8R,9S,10R,11S,13S,14S,17S)-11-(4-(Dimethylamino)phenyl)-17-(3,3-dimethylbut-1-yn-1-yl)-17-hydroxy-13-methyl-1,2,6,7,8,9,10,11,12,13,14,15,16,17-tetradecahydro-3H-cyclopenta[*a*]phenanthren-3-one (3). ¹H NMR (400 MHz, CDCl₃) δ ppm 7.28 (br d, *J* = 8.4 Hz, 2 H), 6.67 (br d, *J* = 8.4 Hz, 2 H), 5.87 (s, 1 H), 3.34 (br t, *J* = 6.0 Hz, 1 H), 2.95 (s, 6 H), 2.80–2.90 (m, 1 H), 2.49–2.57 (m, 1 H), 2.33–2.43 (m, 1 H), 2.22–2.30 (m, 2 H), 2.02–2.22 (m, 4 H), 1.87–1.97 (m, 3 H), 1.68–1.79 (m, 1 H), 1.60–1.67 (m, 1 H), 1.47–1.54 (m, 2 H), 1.38 (ddd, *J* = 11.9, 5.7, 5.7 Hz, 1 H), 1.26–1.30 (m, 1 H), 1.24 (s, 9 H), 0.67 (s, 3 H). *m/z* (ESI, +ve ion) = 474.4 [M + H]⁺.

(8R,9S,10R,11S,13S,14S,17S)-11-(4-(Diethylamino)phenyl)-17-(3,3-dimethylbut-1-yn-1-yl)-17-hydroxy-13-methyl-1,2,6,7,8,9,10,11,12,13,14,15,16,17-tetradecahydro-3H-cyclopenta[*a*]phenanthren-3-one (4). ¹H NMR (400 MHz, CDCl₃) δ ppm 7.23 (br d, *J* = 8.3 Hz, 2 H), 6.60 (br d, *J* = 8.8 Hz, 2 H), 5.86 (br s, 1 H), 3.27–3.39 (m, 5 H), 2.81–2.92 (m, 1 H), 2.47–2.58 (m, 1 H), 2.31–2.43 (m, 1 H), 2.01–2.32 (m, 6 H), 1.86–1.99 (m, 3 H), 1.67–1.77 (m, 1 H), 1.64 (br s, 1 H), 1.45–1.54 (m, 2 H), 1.33–1.42 (m, 1 H), 1.26–1.31 (m, 1 H), 1.24 (s, 9 H), 1.17 (br t, *J* = 6.94 Hz, 6 H), 1.04–1.11 (m, 1 H), 0.67 (s, 3 H). *m/z* (ESI, +ve ion) = 502.4 [M + H]⁺.

(8R,9S,10R,11S,13S,14S,17S)-17-(3,3-Dimethylbut-1-yn-1-yl)-17-hydroxy-13-methyl-11-(4-(morpholinophenyl)-1,2,6,7,8,9,10,11,12,13,14,15,16,17-tetradecahydro-3H-cyclopenta[*a*]phenanthren-3-one (5). ¹H NMR (400 MHz, CDCl₃) δ ppm 7.33 (br d, *J* = 8.3 Hz, 2 H), 6.84 (br d, *J* = 7.5 Hz, 2 H), 5.87 (s, 1 H), 3.88 (br s, 4 H), 3.33–3.42 (m, 1 H), 3.17 (br s, 4 H), 2.77–2.89 (m, 1 H), 2.50–2.59 (m, 1 H), 2.32–2.45 (m, 1 H), 2.03–2.31 (m, 5 H), 1.84–1.99 (m, 3 H), 1.68–1.79 (m, 1 H), 1.63 (s, 1 H), 1.45–1.60 (m, 2 H), 1.25–1.42 (m, 3 H), 1.24 (s, 9 H), 1.07–1.18 (m, 1 H), 0.64 (s, 3 H). *m/z* (ESI, +ve ion) = 516.3 [M + H]⁺.

(8R,9S,10R,11S,13S,14S,17S)-17-(3,3-Dimethylbut-1-yn-1-yl)-17-hydroxy-13-methyl-11-(4-(4-methylpiperazin-1-yl)phenyl)-1,2,6,7,8,9,10,11,12,13,14,15,16,17-tetradecahydro-3H-cyclopenta[*a*]phenanthren-3-one (6). ¹H NMR (400 MHz, CDCl₃) δ ppm 7.30 (d, *J* = 8.8 Hz, 2 H), 6.85 (d, *J* = 8.8 Hz, 2 H), 5.86 (s, 1 H), 3.35 (br t, *J* = 5.8 Hz, 1 H), 3.15–3.26 (m, 4 H), 2.80–2.87 (m, 1 H), 2.58–2.61 (m, 4 H), 2.52–2.56 (m, 1 H), 2.36 (s, 3 H), 2.02–2.29

(m, 6 H), 1.85–1.98 (m, 3 H), 1.66–1.77 (m, 2 H), 1.33–1.54 (m, 3 H), 1.26–1.28 (m, 1 H), 1.24 (s, 9 H), 1.08–1.17 (m, 1 H), 0.64 (s, 3 H). *m/z* (ESI, +ve ion) = 529.4 [M + H]⁺.

(8R,9S,10R,11S,13S,14S,17S)-17-(3,3-Dimethylbut-1-yn-1-yl)-17-hydroxy-13-methyl-11-(4-(4-(methylsulfonyl)piperazin-1-yl)phenyl)-1,2,6,7,8,9,10,11,12,13,14,15,16,17-tetradecahydro-3H-cyclopenta[*a*]phenanthren-3-one (7). ¹H NMR (400 MHz, CDCl₃) δ ppm 7.32–7.35 (m, 2 H), 6.86 (d, *J* = 8.9 Hz, 2 H), 5.87 (s, 1 H), 3.39–3.43 (m, 4 H), 3.35–3.37 (m, 1 H), 3.27–3.29 (m, 4 H), 2.84 (s, 3 H), 2.77–2.83 (m, 1 H), 2.51–2.58 (m, 1 H), 2.33–2.42 (m, 1 H), 2.24–2.30 (m, 2 H), 2.14–2.22 (m, 1 H), 2.03–2.12 (m, 3 H), 1.84–1.96 (m, 3 H), 1.71–1.78 (m, 1 H), 1.62 (s, 3 H), 1.44–1.56 (m, 2 H), 1.34–1.42 (m, 1 H), 1.25–1.29 (m, 1 H), 1.24 (s, 9 H), 1.11–1.18 (m, 1 H), 0.63 (s, 3 H). *m/z* (ESI, +ve ion) = 593.4 [M + H]⁺.

(8R,9S,10R,11S,13S,14S,17S)-11-(4-(Dimethylamino)phenyl)-17-(3,3-dimethylpent-1-yn-1-yl)-17-hydroxy-13-methyl-1,2,6,7,8,9,10,11,12,13,14,15,16,17-tetradecahydro-3H-cyclopenta[*a*]phenanthren-3-one (8). ¹H NMR (400 MHz, CDCl₃) δ ppm 7.25–7.35 (m, 2 H), 6.67 (br d, *J* = 6.4 Hz, 2 H), 5.86 (s, 1 H), 3.31–3.39 (m, 1 H), 2.95 (br s, 6 H), 2.77–2.90 (m, 1 H), 2.49–2.57 (m, 1 H), 2.37 (td, *J* = 14.1, 4.3 Hz, 1 H), 2.27 (dt, *J* = 16.3, 3.9 Hz, 2 H), 2.19 (ddd, *J* = 13.8, 9.6, 5.7 Hz, 1 H), 2.02–2.14 (m, 3 H), 1.87–1.99 (m, 3 H), 1.69–1.78 (m, 1 H), 1.63 (s, 1 H), 1.48–1.54 (m, 2 H), 1.44 (q, *J* = 7.6 Hz, 2 H), 1.33–1.41 (m, 1 H), 1.22–1.31 (m, 1 H), 1.19 (s, 3 H), 1.19 (s, 3 H), 1.10 (br d, *J* = 12.0 Hz, 1 H), 0.99 (t, *J* = 7.6 Hz, 3 H), 0.66 (s, 3 H). *m/z* (ESI, +ve ion) = 488.5 [M + H]⁺.

(8S,9R,10R,11S,13S,14S,17S)-11-(4-(Dimethylamino)phenyl)-17-(3,3-dimethylbut-1-yn-1-yl)-17-hydroxy-10,13-dimethyl-1,2,6,7,8,9,10,11,12,13,14,15,16,17-tetradecahydro-3H-cyclopenta[*a*]phenanthren-3-one (9). Compound 9 was prepared by procedures similar to those described for the synthesis of 15, substituting prop-1-yn-1-ylmagnesium bromide in step 1 with (3,3-dimethylbut-1-yn-1-yl)lithium, which was synthesized from the reaction of *n*-butyllithium with 3,3-dimethylbut-1-yne. ¹H NMR (400 MHz, CDCl₃) δ ppm 7.15–7.41 (br s, 2 H), 6.60 (br d, *J* = 8.6 Hz, 2 H), 5.68 (d, *J* = 1.2 Hz, 1 H), 3.41 (t, *J* = 5.8 Hz, 1 H), 2.93 (s, 6 H), 2.46–2.57 (m, 1 H), 2.11–2.33 (m, 7 H), 1.82–2.04 (m, 3 H), 1.68–1.79 (m, 2 H), 1.35–1.53 (m, 3 H), 1.23 (s, 9 H), 1.05–1.16 (m, 1 H), 1.01 (s, 3 H), 0.88 (s, 3 H). *m/z* (ESI, +ve ion) = 488.5 [M + H]⁺.

(8S,9R,10R,11S,13S,14S,17S)-11-(4-(Dimethylamino)phenyl)-17-hydroxy-10,13-dimethyl-17-(3-methylbut-1-yn-1-yl)-1,2,6,7,8,9,10,11,12,13,14,15,16,17-tetradecahydro-3H-cyclopenta[*a*]phenanthren-3-one (10). Compound 10 was prepared by procedures similar to those described for the synthesis of 15, substituting prop-1-yn-1-ylmagnesium bromide in step 1 with (3-methylbut-1-yn-1-yl)lithium, which was synthesized from the reaction of *n*-butyllithium with 3-methylbut-1-yne. ¹H NMR (400 MHz,

CDCl_3) δ ppm 7.25–7.38 (br s, 2 H), 6.61 (br dd, $J = 6.8, 1.2$ Hz, 2 H), 5.68 (d, $J = 1.3$ Hz, 1 H), 3.37–3.45 (m, 1 H), 2.94 (s, 6 H), 2.61 (dt, $J = 13.7, 6.9$ Hz, 1 H), 2.47–2.56 (m, 1 H), 2.11–2.38 (m, 7 H), 1.83–2.04 (m, 3 H), 1.69–1.78 (m, 2 H), 1.36–1.52 (m, 3 H), 1.18 (d, $J = 6.8$ Hz, 6 H), 1.07–1.15 (m, 1 H), 1.02 (s, 3 H), 0.88 (m, 3 H). m/z (ESI, +ve ion) = 474.4 $[M + H]^+$.

8S,9R,10R,11S,13S,14S,17S)-17-(Cyclopropylethynyl)-11-(4-(dimethylamino)phenyl)-17-hydroxy-10,13-dimethyl-1,2,6,7,8,9,10,11,12,13,14,15,16,17-tetradecahydro-3H-cyclopenta[a]phenanthren-3-one (11). Compound 11 was prepared by procedures similar to those described for the synthesis of 15, substituting prop-1-yn-1-ylmagnesium bromide in step 1 with cyclopropylethynyl lithium, which was synthesized from the reaction of *n*-butyllithium with ethynylcyclopropane. ^1H NMR (400 MHz, CDCl_3) δ ppm 7.15–7.43 (br s, 2 H), 6.60 (br d, $J = 7.3$ Hz, 2 H), 5.68 (d, $J = 1.0$ Hz, 1 H), 3.37–3.46 (m, 1 H), 2.93 (s, 6 H), 2.45–2.58 (m, 1 H), 2.09–2.35 (m, 7 H), 1.84–2.03 (m, 3 H), 1.66–1.81 (m, 2 H), 1.62 (s, 1 H), 1.36–1.54 (m, 3 H), 1.29 (tt, $J = 8.3, 5.0$ Hz, 1 H), 1.09–1.22 (m, 1 H), 1.02 (s, 3 H), 0.87 (s, 3 H), 0.77–0.84 (m, 2 H), 0.64–0.71 (m, 2 H). m/z (ESI, +ve ion) = 472.4 $[M + H]^+$.

8S,9R,10R,11S,13S,14S,17S)-11-(4-(Dimethylamino)phenyl)-17-hydroxy-17-(3-methoxyprop-1-yn-1-yl)-10,13-dimethyl-1,2,6,7,8,9,10,11,12,13,14,15,16,17-tetradecahydro-3H-cyclopenta[a]phenanthren-3-one (12). Compound 12 was prepared by procedures similar to those described for the synthesis of 15, substituting prop-1-yn-1-ylmagnesium bromide in step 1 with (3-methoxyprop-1-yn-1-yl)lithium, which was synthesized from the reaction of *n*-butyllithium with 3-methoxyprop-1-yne. ^1H NMR (400 MHz, CDCl_3) δ ppm 7.15–7.40 (br s, 2 H), 6.52–6.68 (m, 2 H), 5.68 (d, $J = 1.2$ Hz, 1 H), 4.18 (d, $J = 0.88$ Hz, 2 H), 3.41–3.45 (m, 1 H), 3.40 (s, 3 H), 2.94 (s, 6 H), 2.42–2.58 (m, 1 H), 2.20–2.35 (m, 6 H), 2.08–2.17 (m, 1 H), 1.85–2.00 (m, 3 H), 1.72–1.80 (m, 2 H), 1.42–1.53 (m, 3 H), 1.11–1.20 (m, 1 H), 1.02 (3 H, s), 0.90 (3 H, s). m/z (ESI, +ve ion) = 476.4 $[M + H]^+$.

8S,9R,10R,11S,13S,14S,17S)-17-(But-1-yn-1-yl)-11-(4-(dimethylamino)phenyl)-17-hydroxy-10,13-dimethyl-1,2,6,7,8,9,10,11,12,13,14,15,16,17-tetradecahydro-3H-cyclopenta[a]phenanthren-3-one (13). Compound 13 was prepared by procedures similar to those described for the synthesis of 15, substituting prop-1-yn-1-ylmagnesium bromide in step 1 with but-1-yn-1-yl lithium, which was synthesized from the reaction of *n*-butyllithium with but-1-yne. ^1H NMR (400 MHz, CDCl_3) δ ppm 7.22–7.39 (br s, 2 H), 6.61 (br dd, $J = 7.0, 1.5$ Hz, 2 H), 5.68 (d, $J = 1.2$ Hz, 1 H), 3.36–3.47 (m, 1 H), 2.94 (s, 6 H), 2.41–2.60 (m, 1 H), 2.10–2.34 (m, 8 H), 1.82–2.05 (m, 3 H), 1.69–1.80 (m, 2 H), 1.60–1.67 (m, 1 H), 1.43–1.52 (m, 3 H), 1.05–1.20 (m, 4 H), 1.02 (s, 3 H), 0.88 (m, 3 H). m/z (ESI, +ve ion) = 460.4 $[M + H]^+$.

8S,9R,10R,11S,13S,14S,17S)-11-(4-(Dimethylamino)phenyl)-17-hydroxy-10,13-dimethyl-17-(3,3,3-trifluoroprop-1-yn-1-yl)-1,2,6,7,8,9,10,11,12,13,14,15,16,17-tetradecahydro-3H-cyclopenta[a]phenanthren-3-one (14). Compound 14 was prepared by procedures similar to those described for the synthesis of 15, substituting prop-1-yn-1-ylmagnesium bromide in step 1 with (3,3,3-trifluoroprop-1-yn-1-yl)lithium, which was synthesized from the reaction of LDA with 2-bromo-3,3,3-trifluoro-prop-1-ene. ^1H NMR (400 MHz, CDCl_3) δ ppm 7.15–7.40 (br s, 2 H), 6.61 (d, $J = 8.8$ Hz, 2 H), 5.69 (d, $J = 1.3$ Hz, 1 H), 3.45 (br t, $J = 5.9$ Hz, 1 H), 2.94 (s, 6 H), 2.45–2.58 (m, 1 H), 2.22–2.37 (m, 5 H), 2.09–2.19 (m, 2 H), 1.80–2.03 (m, 6 H), 1.30–1.54 (m, 3 H), 1.03 (s, 3 H), 0.92 (s, 3 H). m/z (ESI, +ve ion) = 500.3 $[M + 1]^+$.

8S,9R,10R,11S,13S,14S,17S)-11-(4-(Dimethylamino)phenyl)-17-hydroxy-10,13-dimethyl-17-(prop-1-yn-1-yl)-1,2,6,7,8,9,10,11,12,13,14,15,16,17-tetradecahydro-3H-cyclopenta[a]phenanthren-3-one (15). Step a: (8'S,9'S,10'R,13'S,14'S)-10',13'-Dimethyl-1',2',4',7',8',9',10',12',13',14',15',16'-dodecahydro-11'H-dispiro[1,3]dioxolane-2,3'-cyclopenta[a]phenanthrene-17',2''-[1,3]dioxolan-11'-yl (23). Adrenosterone (22) (50.2 g, 167.1 mmol) was dissolved in DCM (390 mL). Trimethyl orthoformate (91 g, 857.5 mmol) and ethylene glycol (119 g, 1.92 mol) were added successively. Then toluenesulfonic acid (1.9 g, 10.0 mmol) was added. The reaction mixture was heated to 40 °C for 18 h,

and to it was then added pyridine (4 mL). The solution was concentrated, and the residue was extracted with DCM and washed with water. The organic layer was dried with MgSO_4 , filtered, and concentrated to give 74.3 g of crude product, which was recrystallized from hot ethyl acetate to provide 23 (42.3 g, 65%). ^1H NMR (400 MHz, CD_2Cl_2) δ ppm 5.28–5.30 (m, 1 H), 3.76–3.93 (m, 8 H), 2.47–2.62 (m, 3 H), 2.08–2.15 (m, 2 H), 1.95–2.06 (m, 3 H), 1.77–1.93 (m, 6 H), 1.53–1.61 (m, 2 H), 1.31–1.41 (m, 1 H), 1.19 (s, 3 H), 0.78 (s, 3 H). m/z (ESI, +ve ion) 389.3 $(M + H)^+$.

Step b: (8'S,9'S,10'R,13'R,14'S)-10',13'-Dimethyl-1',4',7',8',9',10',13',14',15',16'-decahydro-2'H-dispiro[1,3]dioxolane-2,3'-cyclopenta[a]phenanthrene-17',2''-[1,3]dioxolan-11'-yl 1,1,2,2,3,3,4,4,4-nonafluorobutane-1-sulfonate (24). To an oven-dried 500 mL flask charged with THF (125 mL) and anhydrous diisopropylamine (5.77 mL, 40.9 mmol) was added *n*-butyllithium (1.6 M in hexanes, 25.1 mL, 40.2 mmol) dropwise at –78 °C. The resulting solution was stirred at the same temperature for 25 min. In a separate flask, bis-ketal 23 (3.9 g, 10.0 mmol) was azeotroped from toluene, dried under vacuum, and flushed with argon before it was dissolved in THF (40 mL). This solution was added slowly to the freshly prepared lithium diisopropylamide solution at –78 °C. After the mixture was stirred for 30 min, perfluorobutanesulfonyl fluoride (5.4 mL, 30.1 mmol) was added. The mixture was stirred at the same temperature for another hour before it was allowed to warm to rt. After stirring overnight, additional perfluorobutanesulfonyl fluoride (2.5 mL, 13.9 mmol) was added and the reaction was stirred overnight again. The mixture was quenched with saturated aq NH_4Cl , and the solution was extracted with EtOAc. The organic layer was washed with brine, dried with MgSO_4 , and concentrated. The residue was purified by silica gel column chromatography (gradient elution, 0–20% EtOAc in hexanes) to afford 24 (3.7 g, 55%) as a light yellow solid. ^1H NMR (400 MHz, CDCl_3) δ ppm 6.05 (s, 1 H), 5.51–5.53 (m, 1 H), 3.87–3.99 (m, 8 H), 2.48–2.57 (m, 1 H), 2.39 (d, $J = 8.0$ Hz, 1 H), 2.23–2.31 (m, 1 H), 2.17 (dd, $J = 14.0, 2.8$ Hz, 1 H), 1.63–2.02 (m, 9 H), 1.48–1.59 (m, 1 H), 1.30–1.41 (m, 1 H), 1.16 (s, 3 H), 1.01 (s, 3 H). m/z (ESI, +ve ion) = 671.2 $(M + H)^+$.

Step c: tert-Butyl 4-((8'S,9'S,10'R,13'R,14'S)-10',13'-Dimethyl-1',4',7',8',9',10',13',14',15',16'-decahydro-2'H-dispiro[1,3]dioxolane-2,3'-cyclopenta[a]phenanthrene-17',2''-[1,3]dioxolan-11'-yl)phenyl)(methyl)carbamate (25). A flask was charged with 24 (1.4 g, 2.09 mmol), 4-((tert-butoxycarbonyl)(methyl)amino)phenyl)boronic acid (5.2 g, 20.7 mmol), lithium chloride (177 mg, 4.2 mmol), and $\text{Pd}(\text{PPh}_3)_4$ (193 mg, 0.17 mmol). Then toluene (36 mL), ethanol (18 mL), and aqueous Na_2CO_3 (7.8 mL, 15.6 mmol, 2 M) were added successively and the reaction mixture was degassed with argon. After the mixture was refluxed for 42 h, it was cooled to rt, quenched with aq NaHCO_3 solution, and extracted with EtOAc. The organic layer was washed with brine, dried with MgSO_4 , filtered, and concentrated. Purification of the residue by silica gel column chromatography (gradient elution, 10–15% EtOAc in hexanes) provided 25 (1.1 g, 92%) as a white solid. ^1H NMR (400 MHz, CDCl_3) δ ppm 7.03–7.19 (m, 4 H), 5.81 (d, $J = 1.8$ Hz, 1H), 5.53 (br, d, $J = 5.4$ Hz, 1 H), 3.82–3.98 (m, 8 H), 3.25 (s, 3 H), 2.59 (br, d, $J = 6.4$ Hz, 1 H), 2.42 (br dd, $J = 14.0, 1.8$ Hz, 1 H), 2.11 (dd, $J = 13.8, 3.1$ Hz, 1 H), 1.84–2.06 (m, 6 H), 1.64–1.79 (m, 1 H), 1.48–1.52 (m, 1 H), 1.44 (s, 9 H), 1.25–1.40 (m, 2 H), 1.06 (s, 3 H), 1.07 (s, 3 H), 0.95–1.05 (m, 1 H), 0.82–0.89 (m, 1 H). m/z (ESI, +ve ion) = 578.4 $[M + 1]^+$.

Step d: tert-Butyl 4-((4a'R,5a'S,6a'S,6b'S,9a'R,11a'R,11b'R)-9a',11b'-Dimethyl-1',5a',6',6a',6b',7',8',9a',11a',11b'-decahydro-2'H,4'H-dispiro[1,3]dioxolane-2,3'-cyclopenta[1,2]phenanthro[8a,9-b]oxirene-9',2''-[1,3]dioxolan-11'-yl)phenyl)(methyl)carbamate (26). To a solution of 25 (520 mg, 0.9 mmol) in DCM (10 mL) at 0 °C was added 1,1,1,3,3,3-hexafluoropropan-2-one (0.14 mL, 0.99 mmol), followed by addition of 30% hydrogen peroxide aqueous solution (0.37 mL, 4.5 mmol) and disodium phosphate (383.3 mg, 2.7 mmol). The reaction mixture was stirred at 0 °C for 10 min before it was allowed to warm to rt and stirred for 20 h. Then the same amounts of 1,1,1,3,3,3-hexafluoropropan-2-one, disodium phosphate, and hydrogen peroxide were added, and the reaction was continued stirring. At 27 h, another 0.2 mL of 30%

hydrogen peroxide solution was added and the reaction was allowed to stir overnight. The reaction was quenched at 48 h with 10% Na₂S₂O₃ solution and extracted with EtOAc. The organics were washed with brine, dried with MgSO₄, and concentrated. The residue was purified by silica gel column chromatography (gradient elution, 0–50% EtOAc in hexanes) to provide **26** (470 mg, 88%) as a white foamy solid. ¹H NMR (400 MHz, CDCl₃) δ ppm 7.00–7.21 (m, 4 H), 5.81 (d, *J* = 1.8 Hz, 1 H), 3.76–4.00 (m, 8 H), 3.24 (s, 3 H), 3.00 (d, *J* = 5.3 Hz, 1 H), 2.81 (dd, *J* = 9.4, 1.8 Hz, 1 H), 2.26 (d, *J* = 13.9 Hz, 1 H), 1.90–2.06 (m, 3 H), 1.78–1.90 (m, 2 H), 1.61–1.75 (m, 2 H), 1.50–1.55 (m, 1 H), 1.44 (s, 9 H), 1.25–1.43 (m, 3 H), 1.14–1.18 (m, 1 H), 1.13 (s, 3 H), 1.01 (s, 3 h), 0.63–0.66 (m, 1 H). *m/z* (ESI, +ve ion) = 594.5 [M + 1]⁺.

Step e: *tert*-Butyl 4-((5'*R*,8'*S*,9'*R*,10'*R*,13'*R*,14'*S*)-5'-Hydroxy-10',13'-dimethyl-1',4',5',6',7',8',9',10',13',14',15',16'-dodecahydro-2'*H*-dispiro[[1,3]dioxolane-2,3'-cyclopenta[*a*]phenanthrene-17',2''-[1,3]dioxolan]-11'-yl)phenyl)(methyl)carbamate (**27**). A flask was charged with **26** (2.98 g, 6.02 mmol) and azeotroped from toluene. THF (30 mL) was added. The solution was cooled to –78 °C, and lithium aluminum hydride (1 M solution in THF, 6.02 mL) was added dropwise. Five minutes later, the reaction was allowed to warm to rt and stirred for 1 h. The reaction was quenched with a few drops of methanol, followed by addition of saturated Rochelle's salt solution and EtOAc. The mixture was stirred for 15 min, and the organic layer was separated, washed with brine, dried with MgSO₄, and concentrated. The residue was purified by silica gel column chromatography (gradient elution, 0–50% EtOAc in hexanes) to provide **27** (2.63 g, 88%) as a white solid. ¹H NMR (400 MHz, CDCl₃) δ ppm 7.21 (br dd, *J* = 8.3, 1.8 Hz, 1 H), 6.97–7.14 (m, 3 H), 5.73 (d, *J* = 2.2 Hz, 1 H), 4.28 (br s, 1 H), 3.75–3.97 (m, 8 H), 3.24 (s, 3 H), 3.19–3.23 (m, 1 H), 1.82–2.04 (m, 4 H), 1.62–1.75 (m, 4 H), 1.46–1.52 (m, 3 H), 1.44 (s, 9 H), 1.32–1.42 (m, 2 H), 1.19–1.30 (m, 2 H), 1.03 (s, 3 H), 1.01 (s, 3 H), 0.44–0.54 (m, 1 H). *m/z* (ESI, +ve ion) = 618.3 [M + Na]⁺.

Step f: *tert*-Butyl 4-(((3'*S*,3*b*'*S*,5'*a*'*R*,9'*a*'*R*,9*b*'*S*,9*c*'*R*,10'*a*'*R*,10*b*'*R*)-5'*a*'-Hydroxy-9'*a*'-10*b*'-dimethyl-tetradecahydro-9'*c*'*H*-dispiro[[1,3]dioxolane-2,1'-cyclopenta-1,2]phenanthro[3,4-*b*]oxirene-7',2''-[1,3]dioxolane]-9'*c*'-yl)phenyl)(methyl)carbamate (**28**). 3-Chloroperbenzoic acid (3.57 g, 15.5 mmol, 75% purity) was added to a solution of **27** (1.93 g, 3.88 mmol) in DCM (60 mL). After stirring at rt for 20 h, the reaction was treated with saturated NaHCO₃ and extracted with EtOAc. The organic layer was separated, washed with brine, dried over MgSO₄, and concentrated in vacuo. The residue was purified by silica gel column chromatography (gradient elution, 0–45% EtOAc in hexanes) to provide the desired product **28** (the second eluting isomer, 530 mg, 27%). ¹H NMR (400 MHz, CDCl₃) δ ppm 7.43–7.48 (m, 1 H), 7.05–7.20 (m, 3 H), 4.22 (br s, 1 H), 3.75–4.00 (m, 8 H), 3.22 (s, 3 H), 2.83 (s, 1 H), 2.72 (br d, *J* = 11.0 Hz, 1 H), 2.36 (s, 1 H), 2.08–2.18 (m, 1 H), 1.68–2.01 (m, 5 H), 1.45–1.52 (m, 2 H), 1.43 (s, 9 H), 1.20–1.40 (m, 5 H), 1.13 (s, 3 H), 1.08 (s, 3 H), 0.95–1.05 (m, 1 H), 0.40–0.49 (m, 1 H). *m/z* (ESI, +ve ion) = 634.4 [M + Na]⁺.

Step g: (5'*R*,8'*S*,9'*R*,10'*R*,11'*S*,12'*S*,13'*R*,14'*S*)-10',13'-Dimethyl-11'-(4-(methylamino)phenyl)dodecahydro-2'*H*-dispiro[[1,3]dioxolane-2,3'-cyclopenta[*a*]phenanthrene-17',2''-[1,3]dioxolane]-5',12'(4'*H*)-diol (**29**). An oven-dried 3-necked 250 mL flask was fitted with a coldfinger condenser and an argon balloon. Both the 3-necked flask and the coldfinger were cooled to –78 °C. Liquid ammonia from a supply tank was condensed into the flask until the desired volume of 25 mL was reached. Lithium metal (109 mg, 13.7 mmol) was added, and the solution changed into a dark blue color. The dry ice bath was removed briefly for 2 min to speed up the dissolving process of lithium, then the flask was returned to the cooling bath. Four minutes later, a solution of **28** (1.05 g, 1.72 mmol) in THF (20 mL) was added dropwise in 5 min. The reaction was stirred for 50 min, and its color remained dark blue. At this point, ethanol (0.5 mL) was added, and the mixture was allowed to warm to rt and was quenched with water. EtOAc was added, and air was bubbled into the reaction to purge any residual ammonia. The reaction mixture was further extracted with EtOAc. The organic layer was washed with brine, dried with MgSO₄, concentrated and the residue was purified by silica gel column chromatography (gradient elution, 0–70% EtOAc in

hexanes) to give **29** (715 mg, 81%). ¹H NMR (400 MHz, CDCl₃) δ ppm 7.20–7.31 (br s, 2 H), 6.48–6.51 (m, 2 H), 5.53 (s, 1 H), 4.09 (s, 1 H), 3.81–4.01 (m, 8 H), 3.06 (dd, *J* = 5.9, 1.3 Hz, 1 H), 2.84–2.87 (m, 1 H), 2.83 (s, 3 H), 2.12–2.27 (m, 2 H), 1.80–1.99 (m, 3 H), 1.62–1.78 (m, 5 H), 1.46–1.57 (m, 4 H), 1.30–1.39 (m, 2 H), 0.96 (s, 3 H), 0.80 (s, 3 H). *m/z* (ESI, +ve ion) = 514.4 (M + H)⁺.

Step h: (5'*R*,8'*S*,9'*R*,10'*R*,11'*S*,12'*S*,13'*R*,14'*S*)-11'-(4-(Dimethylamino)phenyl)-10',13'-dimethyl-dodecahydro-2'*H*-dispiro[[1,3]dioxolane-2,3'-cyclopenta[*a*]phenanthrene-17',2''-[1,3]dioxolane]-5',12'(4'*H*)-diol (**30**). To a flask charged with **29** (609 mg, 1.19 mmol) was added DCM (12 mL), followed by addition of acetic acid (0.68 mL, 11.86 mmol) and formaldehyde (0.45 mL, 5.93 mmol). After the mixture was stirred for 6 min, sodium triacetoxyborohydride (276.4 mg, 1.3 mmol) was added. The reaction mixture was stirred for 1 h and then quenched with saturated NaHCO₃ and extracted with EtOAc. The organic layer was dried with MgSO₄ and concentrated. The residue was purified by silica gel chromatography (gradient elution, 30–50% EtOAc in hexanes) to give **30** (575 mg, 92%). ¹H NMR (400 MHz, CDCl₃) δ ppm 7.26–7.38 (br s, 2 H), 6.52–6.60 (m, 1 H), 4.09 (s, 1 H), 3.82–4.01 (m, 8 H), 3.06–3.10 (m, 1 H), 2.92 (s, 6 H), 2.83–2.87 (m, 1 H), 2.09–2.27 (m, 2 H), 1.81–1.99 (m, 3 H), 1.62–1.80 (m, 5 H), 1.45–1.57 (m, 4 H), 1.30–1.40 (m, 2 H), 0.96 (m, 3 H), 0.80 (s, 3 H). *m/z* (ESI, +ve ion) = 528.3 (M + H)⁺.

Step i: (8*S*,9*R*,10*R*,11*S*,12*S*,13*R*,14*S*)-11-(4-(Dimethylamino)phenyl)-12-hydroxy-10,13-dimethyl-1,6,7,8,9,10,11,12,13,14,15,16-dodecahydro-3*H*-cyclopenta[*a*]phenanthrene-3,17(2*H*)-dione (**31**). To a flask charged with **30** (650 mg, 1.23 mmol) was added acetone (15 mL), followed by addition of hydrogen chloride (4 N aqueous solution, 0.92 mL, 3.7 mmol). After the mixture was stirred at rt for 7 h, it was quenched with saturated NaHCO₃ and extracted with EtOAc. The organic layer was washed with brine, dried over MgSO₄, and concentrated in vacuo. The residue was purified by silica gel chromatography (gradient elution, 0–60% EtOAc in hexanes) to provide **31** (501 mg, 96%). ¹H NMR (400 MHz, CDCl₃) δ ppm 7.10–7.40 (m, 2 H), 6.52–6.70 (m, 2 H), 5.69 (d, *J* = 1.2 Hz, 1 H), 4.04 (s, 1 H), 3.33 (br d, *J* = 3.7 Hz, 1 H), 2.94 (s, 6 H), 2.44–2.59 (m, 3 H), 2.20–2.42 (m, 4 H), 1.97–2.11 (m, 3 H), 1.82–1.97 (m, 3 H), 1.66–1.70 (m, 1 H), 1.18–1.33 (m, 1 H), 1.01 (s, 3 H), 0.88 (s, 3 H). *m/z* (ESI, +ve ion) = 422.3 (M + H)⁺.

Step j: *O*-((8*S*,9*R*,10*R*,12*S*,13*R*,14*S*)-11-(4-(Dimethylamino)phenyl)-10,13-dimethyl-3,17-dioxo-2,3,6,7,8,9,10,11,12,13,14,15,16,17-tetradecahydro-1*H*-cyclopenta[*a*]phenanthren-12-yl)-1*H*-imidazole-1-carbothioate (**32**). A flask was charged with **31** (411 mg, 0.97 mmol) and azeotroped from toluene. DCM (24 mL) was added, followed by addition of triethylamine (0.27 mL, 1.95 mmol) and 1,1'-thiocarbonyldiimidazole (2.8 g, 15.6 mmol). After the reaction was stirred at rt for 4 days under argon, it was quenched with diluted 1 N HCl and the solution was extracted with EtOAc. The organic layer was washed with brine, dried with MgSO₄, and concentrated. The residue was purified by silica gel column chromatography (gradient elution, 40–60% EtOAc in hexanes, then 2–6% MeOH in DCM) to give **32** (427 mg, 83%). ¹H NMR (400 MHz, CDCl₃) δ ppm 8.15–8.20 (m, 1 H), 7.45–7.55 (m, 3 H), 7.03 (dd, *J* = 1.8, 0.9 Hz, 1 H), 6.50–6.75 (m, 2 H), 5.83 (d, *J* = 2.1 Hz, 1 H), 5.70 (d, *J* = 1.3 Hz, 1 H), 3.68–3.72 (m, 1 H), 2.97 (s, 6 H), 2.50–2.65 (m, 3 H), 2.31–2.39 (m, 2 H), 2.22–2.26 (m, 2 H), 2.10–2.22 (m, 1 H), 1.63–1.93 (m, 6 H), 1.27–1.32 (m, 1 H), 1.08 (s, 3 H), 1.01 (s, 3 H). *m/z* (ESI, +ve ion) = 554.3 [M + Na]⁺.

Step k: (8*S*,9*R*,10*R*,11*S*,13*S*,14*S*)-11-(4-(Dimethylamino)phenyl)-10,13-dimethyl-1,6,7,8,9,10,11,12,13,14,15,16-dodecahydro-3*H*-cyclopenta[*a*]phenanthrene-3,17(2*H*)-dione (**33**). A flask was charged with **32** (420 mg, 0.79 mmol) and flushed with argon. To the flask was added toluene (19 mL), followed by addition of tributyltin hydride (0.42 mL, 1.58 mmol). After the reaction was heated to reflux for 3 h, it was cooled down to rt and concentrated. The residue was purified by silica gel column chromatography to afford **33** (168 mg, 84%) as a colorless oil. ¹H NMR (400 MHz, CDCl₃) δ ppm 7.14–7.26 (br s, 2 H), 6.60 (br d, *J* = 8.3 Hz, 2 H), 5.68 (d, *J* = 1.3 Hz, 1 H), 3.39 (br t, *J* = 5.6 Hz, 1 H), 2.93 (s, 6 H), 2.41–2.61 (m, 3 H), 2.22–2.34 (m, 4 H), 1.75–2.05 (m, 6 H), 1.64–1.70 (m, 1 H), 1.44–1.50 (m, 1 H),

1.29–1.35 (m, 1 H), 1.14–1.24 (m, 1 H), 1.01 (s, 3 H), 0.88–0.93 (m, 3 H). m/z (ESI, +ve ion) = 406.4 [M + H]⁺.

Step i: 8S,9R,10R,11S,13S,14S,17S)-11-(4-(Dimethylamino)phenyl)-17-hydroxy-10,13-dimethyl-17-(prop-1-yn-1-yl)-1,2,6,7,8,9,10,11,12,13,14,15,16,17-tetradecahydro-3H-cyclopenta[a]phenanthren-3-one (15). A flask was charged with 33 (210 mg, 0.52 mmol) and azeotroped from toluene. To the flask were added *p*-toluenesulfonic acid monohydrate (118.2 mg, 0.62 mmol) and ethanol (8 mL). The reaction was cooled to 0 °C. Triethyl orthoformate (0.26 mL, 1.55 mmol) was added to the mixture, and the reaction was stirred at the same temperature for 1 h. Then triethylamine (0.72 mL) was added to neutralize the acid. The reaction was concentrated and purified by silica gel chromatography (gradient elution, 0–20% EtOAc in hexanes) to provide 34 (66 mg, 29%). m/z (ESI, +ve ion) = 434.4 [M + H]⁺. Ketone 34 (66 mg, 0.15 mmol) was then immediately azeotroped from toluene and flushed with argon. Anhydrous THF (3 mL) was added and the reaction was cooled to 0 °C. Prop-1-yn-1-ylmagnesium bromide (0.5 M in THF, 2.44 mL, 1.22 mmol) was added dropwise and the reaction was allowed to warm to room temperature and stir overnight. The reaction was quenched with saturated NH₄Cl, extracted with EtOAc, and concentrated. The resulting residue was treated with a mixture of THF (1.5 mL), water (1.2 mL), and 4 N HCl (0.75 mL) for 1 h. Saturated NaHCO₃ solution was added to neutralize the HCl, and the mixture was extracted with EtOAc. The organic layer was dried with MgSO₄, concentrated and the residue was purified by reverse phase HPLC (gradient elution, 10–40% with 0.1% TFA in water and 0.1% TFA in ACN as solvents) to give 15 (64 mg, 75%) as a TFA salt. ¹H NMR (400 MHz, CDCl₃) δ ppm 7.35–7.64 (br s, 2 H), 7.11–7.23 (m, 2 H), 5.70 (d, *J* = 1.2 Hz, 1 H), 3.51 (br t, *J* = 5.6 Hz, 1 H), 3.11 (s, 6 H), 2.44–2.61 (m, 1 H), 2.10–2.38 (m, 7 H), 1.90–1.99 (m, 3 H), 1.89 (s, 3 H), 1.67–1.81 (m, 2 H), 1.38–1.57 (m, 3 H), 1.11–1.25 (m, 1 H), 1.00 (s, 3 H), 0.79 (s, 3 H). ¹³C NMR (101 MHz, CDCl₃) δ ppm 199.3, 172.4, 162.7, 144.6, 140.7, 133.2 (2 C), 122.2 (2 C), 82.9, 82.4, 80.7, 56.5, 53.7, 46.2 (2 C), 43.6, 43.4, 40.8, 39.9, 38.7, 35.8, 34.4, 33.7, 33.2, 32.0, 23.1, 22.6, 16.2, 3.9. m/z (ESI, +ve ion) = 446.3 [M + H]⁺.

8S,9R,10R,11S,13S,14S,17S)-17-Hydroxy-11-(4-(isopropyl(methyl)amino)phenyl)-10,13-dimethyl-17-(prop-1-yn-1-yl)-1,2,6,7,8,9,10,11,12,13,14,15,16,17-tetradecahydro-3H-cyclopenta[a]phenanthren-3-one (16). Compound 16 was prepared by procedures similar to those described for the synthesis of 15, substituting formaldehyde with acetone in step h. ¹H NMR (400 MHz, CDCl₃) δ ppm 7.16–7.40 (br s, 2 H), 6.64 (d, *J* = 8.9 Hz, 2 H), 5.67 (d, *J* = 1.3 Hz, 1 H), 4.04–4.11 (m, 1 H), 3.40 (t, *J* = 5.8 Hz, 1 H), 2.70 (s, 3 H), 2.45–2.56 (m, 1 H), 2.10–2.31 (m, 7 H), 1.89–2.00 (m, 3 H), 1.88 (s, 3 H), 1.70–1.78 (m, 3 H), 1.38–1.52 (m, 3 H), 1.16 (d, *J* = 1.4 Hz, 3 H), 1.1 (d, *J* = 1.4 Hz, 3 H), 1.02 (s, 3 H), 0.88 (s, 3 H). m/z (ESI, +ve ion) = 474.4 [M + H]⁺.

8S,9R,10R,11S,13S,14S,17S)-17-Hydroxy-11-(4-((2-methoxyethyl)(methyl)amino)phenyl)-10,13-dimethyl-17-(prop-1-yn-1-yl)-1,2,6,7,8,9,10,11,12,13,14,15,16,17-tetradecahydro-3H-cyclopenta[a]phenanthren-3-one (17). Compound 17 was prepared by procedures similar to those described for the synthesis of 15, substituting formaldehyde in step h with 2-methoxyacetaldehyde, which was formed in situ from the cleavage reaction of 3-methoxypropane-1,2-diol with sodium periodate. ¹H NMR of the TFA salt (400 MHz, CDCl₃) δ ppm 7.40–7.74 (br s, 2 H), 7.28–7.34 (m, 2 H), 5.70–5.74 (m, 1 H), 3.37–3.67 (m, 5 H), 3.26 (s, 3 H), 3.22 (br s, 3 H), 2.38–2.58 (m, 1 H), 2.13–2.41 (m, 7 H), 1.86–2.01 (m, 3 H), 1.89 (s, 3 H), 1.71–1.83 (m, 2 H), 1.39–1.58 (m, 3 H), 1.12–1.26 (m, 1 H), 1.01 (s, 3 H), 0.77 (s, 3 H). m/z (ESI, +ve ion) = 490.4 [M + H]⁺.

8S,9R,10R,11S,13S,14S,17S)-17-Hydroxy-10,13-dimethyl-17-(prop-1-yn-1-yl)-11-(4-(pyrrolidin-1-yl)phenyl)-1,2,6,7,8,9,10,11,12,13,14,15,16,17-tetradecahydro-3H-cyclopenta[a]phenanthren-3-one (18). Compound 18 was prepared by procedures similar to those described for the synthesis of 15, substituting 4-((*tert*-butoxycarbonyl)(methyl)amino)phenylboronic acid in step c with 4-((*tert*-butoxycarbonyl)amino)phenylboronic acid and formaldehyde in step h with succinaldehyde, which was formed in situ from the hydrolysis reaction of 2,5-dimethoxy-

tetrahydrofuran with sulfuric acid. ¹H NMR (400 MHz, CDCl₃) δ ppm 7.20–7.38 (br s, 2 H), 6.43 (d, *J* = 8.8 Hz, 2 H), 5.67 (d, *J* = 1.3 Hz, 1 H), 3.40 (br t, *J* = 5.8 Hz, 1 H), 3.24–3.32 (m, 4 H), 2.46–2.58 (m, 1 H), 2.10–2.32 (m, 7 H), 1.97–2.03 (m, 4 H), 1.84–1.96 (m, 3 H), 1.89 (s, 3 H), 1.69–1.78 (m, 2 H), 1.66 (s, 1 H), 1.37–1.52 (m, 3 H), 1.10–1.21 (m, 1 H), 1.03 (s, 3 H), 0.90 (s, 3 H). m/z (ESI, +ve ion) = 472.4 [M + H]⁺.

8S,9R,10R,11S,13S,14S,17S)-11-(4-(1H-Pyrrol-1-yl)phenyl)-17-hydroxy-10,13-dimethyl-17-(prop-1-yn-1-yl)-1,2,6,7,8,9,10,11,12,13,14,15,16,17-tetradecahydro-3H-cyclopenta[a]phenanthren-3-one (19). Compound 19 was prepared by procedures similar to those described for the synthesis of 18. Reductive amination of 29 with succinaldehyde in step h provided 4-pyrrolidinylphenyl-substituted intermediate used in the synthesis of 18 and 4-pyrrolylphenyl-substituted intermediate as a byproduct. The latter was used in step i for the synthesis of 19. ¹H NMR (400 MHz, CDCl₃) δ ppm 7.35–7.61 (br s, 2 H), 7.23–7.27 (m, 2 H), 7.09 (t, *J* = 2.2 Hz, 2 H), 6.34 (t, *J* = 2.2 Hz, 2 H), 5.70 (d, *J* = 1.0 Hz, 1 H), 3.54 (br t, *J* = 5.9 Hz, 1 H), 2.53 (td, *J* = 14.5, 4.5 Hz, 1 H), 2.14–2.38 (m, 7 H), 1.91–2.01 (m, 3 H), 1.90 (s, 3 H), 1.75–1.83 (m, 2 H), 1.72 (s, 1 H), 1.40–1.58 (m, 3 H), 1.13–1.24 (m, 1 H), 1.06 (s, 3 H), 0.85 (s, 3 H). m/z (ESI, +ve ion) = 468.4 [M + H]⁺.

8S,9R,10R,11S,13S,14S,17S)-17-Hydroxy-11-(4-methoxyphenyl)-10,13-dimethyl-17-(prop-1-yn-1-yl)-1,2,6,7,8,9,10,11,12,13,14,15,16,17-tetradecahydro-3H-cyclopenta[a]phenanthren-3-one (20). Compound 20 was prepared by procedures similar to those described for the synthesis of 15, substituting 4-((*tert*-butoxycarbonyl)(methyl)amino)phenylboronic acid in step c with 4-methoxyphenylboronic acid. ¹H NMR (400 MHz, CD₂Cl₂) δ ppm 7.15–7.51 (br s, 2 H), 6.67–6.83 (m, 2 H), 5.65 (d, *J* = 1.3 Hz, 1 H), 3.77 (s, 3 H), 3.45 (br t, *J* = 5.7 Hz, 1 H), 2.42–2.59 (m, 1 H), 2.20–2.34 (m, 6 H), 2.09–2.19 (m, 2 H), 1.86–1.95 (m, 2 H), 1.85 (s, 3 H), 1.71–1.79 (m, 1 H), 1.64–1.70 (m, 1 H), 1.33–1.55 (m, 3 H), 1.06–1.19 (m, 1 H), 0.98 (s, 3 H), 0.80 (s, 3 H). m/z (ESI, +ve ion) = 433.4 [M + H]⁺.

(8S,9S,10R,11S,13S,14S,17S)-11-((4-Chlorobenzyl)oxy)-17-hydroxy-10,13-dimethyl-17-(prop-1-yn-1-yl)-1,2,6,7,8,9,10,11,12,13,14,15,16,17-tetradecahydro-3H-cyclopenta[a]phenanthren-3-one (21). Step a: (8'S,9'S,10'R,11'S,13'S,14'S)-10',13'-Dimethyl-1',4',7',8',9',10',11',12',13',14',15',16'-dodecahydro-2'H-dispiro[[1,3]dioxolane-2,3'-cyclopenta[a]phenanthrene-17',2''-[1,3]dioxolan]-11'-ol (35). A flask was charged with 23 (2.0 g, 5.15 mmol) and azeotroped from toluene. The flask was under high vacuum for 30 min and then flushed with argon. After anhydrous THF (15 mL) was added and the reaction was cooled to 0 °C, lithium aluminum hydride (1 M solution in THF, 5.15 mL, 5.15 mmol) was added dropwise. The reaction was allowed to warm to rt and stirred for 3 h. Then the reaction was cooled to 0 °C and quenched with 0.4 mL of MeOH, followed by addition of saturated Rochelle's salt solution and EtOAc. The mixture was stirred for 15 min, and the organic layer was separated. The aqueous layer was extracted with EtOAc, and the combined organic layers were washed with brine, dried with MgSO₄ and concentrated. The residue was purified by silica gel column chromatography (gradient elution, 15–40% EtOAc in hexanes) to provide 35 (1.23 g, 61%) as a white solid. ¹H NMR (400 MHz, CDCl₃) δ ppm 5.23–5.26 (m, 1 H), 4.42–4.51 (m, 1 H), 3.79–4.01 (m, 8 H), 2.62 (br dd, *J* = 14.4, 2.4 Hz, 1 H), 1.80–2.20 (m, 7 H), 1.62–1.78 (m, 3 H), 1.58 (br dd, *J* = 13.9, 2.3 Hz, 1 H), 1.34–1.53 (m, 3 H), 1.29 (s, 3 H), 1.20 (br dd, *J* = 11.8, 3.9 Hz, 1 H), 1.11 (s, 3 H), 1.05 (br d, *J* = 3.7 Hz, 1 H). m/z (ESI, +ve ion) = 391.3 [M + H]⁺.

Step b: (8'S,9'S,10'R,11'S,13'S,14'S)-11'-((4-Chlorobenzyl)oxy)-10',13'-dimethyl-1',4',7',8',9',10',11',12',13',14',15',16'-dodecahydro-2'H-dispiro[[1,3]dioxolane-2,3'-cyclopenta[a]phenanthrene-17',2''-[1,3]dioxolane] (36). A flask was charged with 35 (695 mg, 1.78 mmol) and azeotroped from toluene. The flask was put on high vacuum pump for 30 min and then flushed with argon. After DMF (12 mL) was added and the reaction was cooled to 0 °C, sodium hydride (170.9 mg, 4.27 mmol) was added. The reaction was allowed to warm to rt and stirred for 25 min. Then a 2.5 mL DMF solution of 4-chlorobenzyl bromide (1.28 g, 6.23 mmol) was added

dropwise. The reaction was stirred overnight and quenched with saturated NH_4Cl . The solution was extracted with EtOAc, and the organic layer was washed with brine, dried with MgSO_4 , and concentrated. The residue was purified by silica gel column chromatography (gradient elution, 0–40% EtOAc in hexanes) to provide **36** (625 mg, 68%) as a foamy white solid. $^1\text{H NMR}$ (400 MHz, CDCl_3) δ ppm 7.24–7.33 (m, 4 H), 5.23 (dt, $J = 4.4, 2.3$ Hz, 1 H), 4.66 (d, $J = 11.4$ Hz, 1 H), 4.19 (d, $J = 8.0$ Hz, 1 H), 4.02–4.05 (m, 1 H), 3.82–3.99 (m, 8 H), 2.53–2.64 (m, 1 H), 2.07–2.22 (m, 2 H), 1.91–2.04 (m, 3 H), 1.64–1.84 (m, 6 H), 1.41–1.56 (m, 3 H), 1.32–1.41 (m, 1 H), 1.26–1.29 (m, 1 H), 1.20 (s, 3 H), 1.08 (s, 3 H). m/z (ESI, +ve ion) = 515.2 $[\text{M} + \text{H}]^+$.

Step c: (8S,9S,10R,11S,13S,14S)-11-((4-Chlorobenzyl)oxy)-10,13-dimethyl-1,6,7,8,9,10,11,12,13,14,15,16-dodecahydro-3H-cyclopenta[*a*]phenanthrene-3,17(2H)-dione (37). To a flask charged with **36** was added acetone (11 mL), followed by addition of 4 N HCl (0.61 mL, 2.43 mmol). After the mixture was stirred at rt for 2.5 h, it was quenched with saturated NaHCO_3 solution, concentrated to remove acetone, and extracted with EtOAc. The organic layer was washed with brine, dried with anhydrous sodium sulfate, and concentrated. The residue was purified by silica gel column chromatography (gradient elution, 0–40% EtOAc in hexanes) to provide **37** (446 mg, 86%) as a white solid. $^1\text{H NMR}$ (400 MHz, CDCl_3) δ ppm 7.31–7.35 (m, 2 H), 7.23–7.27 (m, 2 H), 5.70 (d, $J = 1.6$ Hz, 1 H), 4.68 (d, $J = 11.3$ Hz, 1 H), 4.26 (d, $J = 11.1$ Hz, 1 H), 4.04–4.08 (m, 1 H), 2.39–2.58 (m, 4 H), 2.18–2.38 (m, 3 H), 1.95–2.18 (m, 5 H), 1.77–1.87 (m, 1 H), 1.62–1.72 (m, 1 H), 1.37 (s, 3 H), 1.23–1.32 (m, 1 H), 1.15–1.22 (m, 1 H), 1.12 (s, 3 H), 1.05–1.11 (m, 1 H). m/z (ESI, +ve ion) = 427.3 $[\text{M} + \text{H}]^+$.

Step d: (8S,9S,10R,11S,13S,14S,17S)-11-((4-Chlorobenzyl)oxy)-17-hydroxy-10,13-dimethyl-17-(prop-1-yn-1-yl)-1,2,6,7,8,9,10,11,12,13,14,15,16,17-tetradecahydro-3H-cyclopenta[*a*]phenanthren-3-one (21). To a flask charged with **37** (92 mg, 0.22 mmol) and *p*-toluenesulfonic acid monohydrate (4.1 mg, 0.02 mmol) were added THF (2.1 mL) and ethanol (0.07 mL), followed by addition of triethyl orthoformate (0.08 mL, 0.47 mmol) under argon. After the reaction was stirred at rt for 3 h, it was quenched with saturated NaHCO_3 and extracted with EtOAc. The organic layer was dried with MgSO_4 and concentrated. The residue was purified by silica gel chromatography (gradient elution, 0–20% EtOAc in hexanes) to provide the ethoxy enol ether (**38**) (55 mg, 56%) as an oil. m/z (ESI, +ve ion) = 455.3 $[\text{M} + \text{H}]^+$. Compound **38** was immediately azeotroped from toluene and flushed with argon. Anhydrous THF (1.5 mL) was added, and the reaction mixture was cooled to 0 °C. Prop-1-yn-1-ylmagnesium bromide (1.93 mL, 0.97 mmol) was added dropwise. The reaction was allowed to warm to rt and stirred overnight. The reaction was quenched with saturated NH_4Cl and extracted with EtOAc. The organic layer was concentrated, and the residue was dissolved in THF (2 mL) and 1 N HCl (1.5 mL). After the mixture was stirred at rt for 30 min, it was quenched with saturated NaHCO_3 and extracted with EtOAc. The organic layer was dried with MgSO_4 , concentrated and the residue was purified by silica gel column chromatography (gradient elution, 0–40% EtOAc in hexanes) to provide **21** (43 mg, 76%) as a white solid. $^1\text{H NMR}$ (400 MHz, CDCl_3) δ ppm 7.30–7.34 (m, 2 H), 7.25–7.29 (m, 2 H), 5.67–5.69 (m, 1 H), 4.68 (d, $J = 11.3$ Hz, 1 H), 4.21 (d, $J = 11.3$ Hz, 1 H), 4.04–4.07 (m, 1 H), 2.30–2.50 (m, 3 H), 2.19–2.29 (m, 3 H), 1.95–2.06 (m, 4 H), 1.85–1.89 (m, 1 H), 1.87 (s, 3 H), 1.68–1.75 (m, 1 H), 1.59–1.64 (m, 1 H), 1.40–1.46 (m, 2 H), 1.35 (s, 3 H), 1.10 (s, 3 H), 1.05–1.13 (m, 2 H). m/z (ESI, +ve ion) = 467.3 $[\text{M} + \text{H}]^+$.

■ ASSOCIATED CONTENT

Supporting Information

The Supporting Information is available free of charge on the ACS Publications website at DOI: 10.1021/acs.jmedchem.9b00711.

Molecular formula strings (CSV)

In vitro biological assays, in vivo study protocols, HPLC profile of compound **15**, determination of the single crystal structures of **1** and **15** (PDF)

■ AUTHOR INFORMATION

Corresponding Authors

*X.D.: (phone, office) 650-388-5602; (e-mail) xiaohui.du@oricpharma.com.

*D.S.: (phone, office) 650-388-5607; (e-mail) daqing.sun@oricpharma.com.

ORCID

Xiaohui Du: 0000-0001-5444-9434

Yosup Rew: 0000-0003-1155-4298

Notes

The authors declare no competing financial interest. CIF files of **1** and **15** have been deposited with Cambridge Crystallographic Data Centre (CCDC).

■ ACKNOWLEDGMENTS

We thank Dr. Omar Kabbarah and Dr. Brian Blank for critical reading of our manuscript.

■ ABBREVIATIONS USED

ACN, acetonitrile; HOAc, acetic acid; AR, androgen receptor; CL, clearance; CMC, carboxymethyl cellulose; CRPC, castration-resistant prostate cancer; CYP3A4, cytochrome P450 3A4; CYP 2C8, cytochrome P450 2C8; DCM, dichloromethane; D5W, dextrose 5% in water; DMA, dimethylacetamide; DMSO, dimethyl sulfoxide; EtOAc, ethyl acetate; FKBP5, FK506 binding protein 5; GR, glucocorticoid receptor; HPMC, hydroxypropyl methylcellulose; IPA, isopropyl alcohol; LDA, lithium diisopropylamide; LUC, luciferase; PEG, polyethylene glycol; PR, progesterone receptor; TsOH, *p*-toluenesulfonic acid; QD, once a day dosing; RT-qPCR, quantitative reverse transcription polymerase chain reaction; SEM, standard error of mean; TFA, trifluoroacetic acid; THF, tetrahydrofuran; Tween 80, polyoxyethylene (20) sorbitan monooleate.

■ REFERENCES

- (1) Busada, J. T.; Cidlowski, J. A. Mechanisms of glucocorticoid action during development. *Curr. Top. Dev. Biol.* **2017**, *125*, 147–170.
- (2) Zhou, J.; Cidlowski, J. A. The human glucocorticoid receptor: one gene, multiple proteins and diverse responses. *Steroids* **2005**, *70*, 407–417.
- (3) Adcock, I. M. Molecular mechanisms of glucocorticosteroid actions. *Pulm. Pharmacol. Ther.* **2000**, *13*, 115–126.
- (4) Raff, H.; Carroll, T. Cushing's syndrome: from physiological principles to diagnosis and clinical care. *J. Physiol.* **2015**, *593* (3), 493–506.
- (5) Ferris, H. A.; Kahn, C. R. New mechanisms of glucocorticoid-induced insulin resistance: make no bones about it. *J. Clin. Invest.* **2012**, *122*, 3854–3857.
- (6) Yin, H.; Galfalvy, H.; Pantazatos, S. P.; Huang, Y.-y.; Rosoklija, G. B.; Dwork, A. J.; Burke, A.; Arango, V.; Oquendo, M. A.; Mann, J. J. Glucocorticoid receptor-related genes: genotype and brain gene expression relationships to suicide and major depressive disorder. *Depression Anxiety* **2016**, *33*, 531–540.
- (7) Azher, S.; Azami, O.; Amato, C.; McCullough, M.; Celentano, A.; Cirillo, N. The non-conventional effects of glucocorticoids in cancer. *J. Cell. Physiol.* **2016**, *231*, 2368–2373.
- (8) Coutinho, A. E.; Chapman, K. E. The anti-inflammatory and immunosuppressive effects of glucocorticoids, recent developments and mechanistic insights. *Mol. Cell. Endocrinol.* **2011**, *335*, 2–13.

- (9) Clark, R. D. Glucocorticoid receptor antagonists. *Curr. Top. Med. Chem.* **2008**, *8*, 813–838.
- (10) Fleseriu, M.; Molitch, M. E.; Gross, C.; Schteingart, D. E.; Vaughan, T. B., 3rd; Biller, B. M. A new therapeutic approach in the medical treatment of Cushing's syndrome: glucocorticoid receptor blockade with mifepristone. *Endocr Pract* **2013**, *19*, 313–326.
- (11) Volden, P. A.; Conzen, S. D. The influence of glucocorticoid signaling on tumor progression. *Brain, Behav., Immun.* **2013**, *30* (Suppl), S26–S31.
- (12) Stringer-Reasor, E. M.; Baker, G. M.; Skor, M. N.; Kocherginsky, M.; Lengyel, E.; Fleming, G. F.; Conzen, S. D. Glucocorticoid receptor activation inhibits chemotherapy-induced cell death in high-grade serous ovarian carcinoma. *Gynecol. Oncol.* **2015**, *138*, 656–662.
- (13) Skor, M. N.; Wonder, E. L.; Kocherginsky, M.; Goyal, A.; Hall, B. A.; Cai, Y.; Conzen, S. D. Glucocorticoid receptor antagonism as a novel therapy for triple-negative breast cancer. *Clin. Cancer Res.* **2013**, *19*, 6163–6172.
- (14) Liu, L.; Aleksandrowicz, E.; Schonsiegel, F.; Groner, D.; Bauer, N.; Nwaeburu, C. C.; Zhao, Z.; Gladkich, J.; Hoppe-Tichy, T.; Yefenof, E.; Hackert, T.; Strobel, O.; Herr, I. Dexamethasone mediates pancreatic cancer progression by glucocorticoid receptor, TGF β and JNK/AP-1. *Cell Death Dis.* **2017**, *8*, e3064.
- (15) Ge, H.; Ni, S.; Wang, X.; Xu, N.; Liu, Y.; Wang, X.; Wang, L.; Song, D.; Song, Y.; Bai, C. Dexamethasone reduces sensitivity to cisplatin by blunting p53-dependent cellular senescence in non-small cell lung cancer. *PLoS One* **2012**, *7*, e51821.
- (16) Zhang, C.; Mattern, J.; Haferkamp, A.; Pfitzenmaier, J.; Hohenfellner, M.; Rittgen, W.; Edler, L.; Debatin, K. M.; Groene, E.; Herr, I. Corticosteroid-induced chemotherapy resistance in urological cancers. *Cancer Biol. Ther.* **2006**, *5*, 59–64.
- (17) Arora, V. K.; Schenkein, E.; Murali, R.; Subudhi, S. K.; Wongvipat, J.; Balbas, M. D.; Shah, N.; Cai, L.; Efstathiou, E.; Logothetis, C.; Zheng, D.; Sawyers, C. L. Glucocorticoid receptor confers resistance to antiandrogens by bypassing androgen receptor blockade. *Cell* **2013**, *155*, 1309–1322.
- (18) Kroon, J.; Pühr, M.; Buijs, J. T.; van der Horst, G.; Hemmer, D. M.; Marijt, K. A.; Hwang, M. S.; Masood, M.; Grimm, S.; Storm, G.; Metselaar, J. M.; Meijer, O. C.; Culig, Z.; van der Pluijm, G. Glucocorticoid receptor antagonism reverts docetaxel resistance in human prostate cancer. *Endocr.-Relat. Cancer* **2016**, *23*, 35–45.
- (19) Szmulewitz, R. Z.; Nabhan, C.; O'Donnell, P. H.; Kach, J.; Karrison, T.; Martinez, E.; Stadler, W. M. A phase I/II trial of enzalutamide plus the glucocorticoid receptor antagonist mifepristone for patients with metastatic castration-resistant prostate cancer (mCRPC). *J. Clin. Oncol.* **2016**, *34* (15 Suppl.), TPS5091.
- (20) Nanda, R.; Stringer-Reasor, E. M.; Saha, P.; Kocherginsky, M.; Gibson, J.; Libao, B.; Hoffman, P. C.; Obeid, E.; Merkel, D. E.; Khrantsova, G.; Skor, M.; Krausz, T.; Cohen, R. N.; Ratain, M. J.; Fleming, G. F.; Conzen, S. D. A randomized phase I trial of nanoparticle albumin-bound paclitaxel with or without mifepristone for advanced breast cancer. *SpringerPlus* **2016**, *5*, 947.
- (21) Spitz, I. M.; Bardin, C. W. Mifepristone (RU 486)—a modulator of progestin and glucocorticoid action. *N. Engl. J. Med.* **1993**, *329*, 404–412.
- (22) Johanssen, S.; Alloio, B. Mifepristone (RU 486) in Cushing's syndrome. *Eur. J. Endocrinol.* **2007**, *157*, 561–569.
- (23) Zhou, H.; Jachan, N.; Tran, C.; McWeeney, D.; Balbas, M.; Schenkein, E.; Sutimantanapi, D.; Zovorotinskaya, T.; Jackson, E.; Medina, J.; Sun, D.; Rew, Y.; Du, X.; Yan, X.; Zhu, L.; Ye, Q.; Singh, M.; Fantin, V. Activation of AR signaling by mifepristone enhances prostate cancer growth and impairs enzalutamide response. *Proc. Am. Assoc. Cancer Res.* **2017**, *58*, 1066.
- (24) Rew, Y.; Du, X.; Eksterowicz, J.; Zhou, H.; Jahchan, N.; Zhu, L.; Yan, X.; Kawai, H.; McGee, L. R.; Medina, J. C.; Huang, T.; Chen, C.; Zavorotinskaya, T.; Sutimantanapi, D.; Waszczuk, J.; Jackson, E.; Huang, E.; Ye, Q.; Fantin, V. R.; Sun, D. Discovery of a potent and selective steroidal glucocorticoid receptor antagonist (ORIC-101). *J. Med. Chem.* **2018**, *61*, 7767–7784.
- (25) Cleve, A.; Fritzemeier, K.; Heinrich, N.; Klar, U.; Müller-Fahrnow, A.; Neef, G.; Ottow, E.; Schwede, W. 11 β -Aryl steroids in the androstene series. The role of the 11 β -region in steroid progesterone receptor interaction. *Tetrahedron* **1996**, *52*, 1529–1542.
- (26) The small molecule structure of mifepristone was also compared with the cocrystal structure of mifepristone bound to PR, and the two structures are very similar (not shown) indicating that mifepristone binds in a low energy conformation to PR. In addition, ab initio calculations were performed to compare **3** with **15**. The C9–C10 double bond has been reduced in **3**, and this allows for a more direct evaluation of the effect of adding the C10 methyl group to the scaffold. The results are in line with the comparison of **1** and **15** in that the C₉–C₁₁–C₂₁–C₂₂ torsional angle is predicted to be larger for **15** (38.8°) than for **1** (26.7°). The result for **15** also shows good agreement between the calculation and small molecule X-ray structure, suggesting that crystal packing is not an issue in the small molecule X-ray.
- (27) Jin, Z.; Lin, H.; Srinivasan, S.; Nwachukwu, J. C.; Bruno, N.; Griffin, P. R.; Nettles, K. W.; Kamenecka, T. M. Synthesis of novel steroidal agonists, partial agonists, and antagonists for the glucocorticoid receptor. *Bioorg. Med. Chem. Lett.* **2017**, *27*, 347–353.
- (28) Sitruk-Ware, R.; Spitz, I. M. Pharmacological properties of mifepristone: toxicology and safety in animal and human studies. *Contraception* **2003**, *68*, 409–420.
- (29) (a) Biloski, A. J.; Heggs, R. P.; Ganem, B. Catalytic epoxidation of alkenes with hexafluoroacetone/hydrogen peroxide: 4,4-dimethyl-3,5,8-trioxabicyclo[5.1.0]octane. *Synthesis* **1980**, *1980*, 810–811. (b) van Vliet, M. C. A.; Arends, I. W. C. E.; Sheldon, R. A. Hexafluoroacetone in Hexafluoro-2-propanol: A highly active medium for epoxidation with aqueous hydrogen peroxide. *Synlett* **2001**, *2001*, 1305–1307. (c) Kim, H. K.; Blye, R. P.; Rao, P. N.; Cessac, J. W.; Acosta, C. K.; Simmons, A. M. Structural Modification of 19-Norprogesterone I: 17- α -Substituted, 11- β -Substituted-4-Aryl and 21-Substituted 19-Norpregnadienedione as New Antiprogestational Agents. US6,900,193B1, 2005.
- (30) Ottow, E.; Rohde, R.; Schwede, W.; Wiechert, R. Synthesis of 11 β -(alkynyl)-substituted 19-norsteroids. *Tetrahedron Lett.* **1993**, *34*, 5253–5256.
- (31) Gioiello, A.; Sardella, R.; Rosatelli, E.; Sadeghpour, B. M.; Natalini, B.; Pellicciari, R. Novel stereoselective synthesis and chromatographic evaluation of E-guggulsterone. *Steroids* **2012**, *77*, 250–254.
- (32) Compound **15** is also selective against mineralocorticoid receptor (MR). It neither induces nor inhibits aldosterone-induced interaction between MR and the steroid receptor coactivator at the concentration of 5 μ M.